



**Intel® Model: 11000D2W, FCC ID: PD911000D2**

**Intel model 11000D2W embedded inside Lenovo model TP00082A**

**WiGig subsystem – Power Density Test Report**

---

*May 2016*

*Revision 1.3*



**Notice:** This document contains information on products in the design phase of development. The information here is subject to change without notice. Do not finalize a design with this information.

INFORMATION IN THIS DOCUMENT IS PROVIDED IN CONNECTION WITH INTEL PRODUCTS. NO LICENSE, EXPRESS OR IMPLIED, BY ESTOPPEL OR OTHERWISE, TO ANY INTELLECTUAL PROPERTY RIGHTS IS GRANTED BY THIS DOCUMENT. EXCEPT AS PROVIDED IN INTEL'S TERMS AND CONDITIONS OF SALE FOR SUCH PRODUCTS, INTEL ASSUMES NO LIABILITY WHATSOEVER AND INTEL DISCLAIMS ANY EXPRESS OR IMPLIED WARRANTY, RELATING TO SALE AND/OR USE OF INTEL PRODUCTS INCLUDING LIABILITY OR WARRANTIES RELATING TO FITNESS FOR A PARTICULAR PURPOSE, MERCHANTABILITY, OR INFRINGEMENT OF ANY PATENT, COPYRIGHT OR OTHER INTELLECTUAL PROPERTY RIGHT.

A "Mission Critical Application" is any application in which failure of the Intel Product could result, directly or indirectly, in personal injury or death. SHOULD YOU PURCHASE OR USE INTEL'S PRODUCTS FOR ANY SUCH MISSION CRITICAL APPLICATION, YOU SHALL INDEMNIFY AND HOLD INTEL AND ITS SUBSIDIARIES, SUBCONTRACTORS AND AFFILIATES, AND THE DIRECTORS, OFFICERS, AND EMPLOYEES OF EACH, HARMLESS AGAINST ALL CLAIMS COSTS, DAMAGES, AND EXPENSES AND REASONABLE ATTORNEYS' FEES ARISING OUT OF, DIRECTLY OR INDIRECTLY, ANY CLAIM OF PRODUCT LIABILITY, PERSONAL INJURY, OR DEATH ARISING IN ANY WAY OUT OF SUCH MISSION CRITICAL APPLICATION, WHETHER OR NOT INTEL OR ITS SUBCONTRACTOR WAS NEGLIGENT IN THE DESIGN, MANUFACTURE, OR WARNING OF THE INTEL PRODUCT OR ANY OF ITS PARTS.

Intel may make changes to specifications and product descriptions at any time, without notice. Designers must not rely on the absence or characteristics of any features or instructions marked "reserved" or "undefined." Intel reserves these for future definition and shall have no responsibility whatsoever for conflicts or incompatibilities arising from future changes to them. The information here is subject to change without notice. Do not finalize a design with this information.

Intel software products are copyrighted by and shall remain the property of Intel Corporation. Use, duplication, or disclosure is subject to restrictions stated in Intel's Software License Agreement, or in the case of software delivered to the government, in accordance with the software license agreement as defined in FAR 52.227-7013.

The products described in this document may contain design defects or errors known as errata which may cause the product to deviate from published specifications. Current characterized errata are available on request.

The code names presented in this document are only for use by Intel to identify products, technologies, or services in development that have not been made commercially available to the public, i.e., announced, launched, or shipped. They are not "commercial" names for products or services and are not intended to function as trademarks.

Contact your local Intel sales office or your distributor to obtain the latest specifications and before placing your product order.

Copies of documents which have an order number and are referenced in this document, or other Intel literature may be obtained by calling 1-800-548-4725 or by visiting Intel's website at <http://www.intel.com/design/literature.htm>.

Intel processor numbers are not a measure of performance. Processor numbers differentiate features within each processor family, not across different processor families. See [http://www.intel.com/products/processor\\_number](http://www.intel.com/products/processor_number) for details.

Intel is a trademark of Intel Corporation or in the US and other countries.

\* Other brands and names may be claimed as the property of others.

Copyright © 2015 Intel Corporation. All rights reserved.



## Table of Contents

<b>1</b>	<b>Document Scope</b> .....	<b>7</b>
<b>2</b>	<b>Background – WiGig System Operation</b> .....	<b>8</b>
2.1	System Block Diagram .....	8
2.2	Beam Forming.....	8
2.3	TX Duty Cycle .....	9
2.4	Intel 11000D2W Module In Lenovo Model TP00082A .....	9
<b>3</b>	<b>Simulation Methodology</b> .....	<b>10</b>
3.1	Assessment Considerations .....	10
3.2	Establishing worst case near-field test configuration .....	10
3.3	Simulation tool .....	10
3.3.1	Tool description.....	10
3.3.2	Solver description.....	10
3.3.3	Convergence criteria and Power Density Calculations .....	11
3.4	Finding near field worst case simulation configuration .....	11
3.4.1	Terminology: .....	12
3.4.2	Primer on field vector representation: .....	13
3.4.3	Domain search for worst case direction.....	15
3.5	3D Models Used In the Simulation .....	17
3.5.1	RFEM Housing Inside Intel 11000D2W Module .....	17
3.5.2	Closest Distance To The Body Of An End User.....	17
3.5.3	Metals In Proximity Of The RFEM .....	18
3.6	Antenna Feed.....	18
<b>4</b>	<b>Simulation Results</b> .....	<b>19</b>
4.1	Upper bound simulation results.....	19
4.2	Spot power density values with worst antenna phases.....	23
4.3	One dimensional cut of the mesh spot power density .....	27
4.4	Integrated power density over 1cm <sup>2</sup> .....	29
4.5	Power density VS distance .....	31
<b>5</b>	<b>Validation Simulation Model in Near- Field to Far-Field</b> .....	<b>34</b>
5.1	Correlation of EIRP in the Near to Far Field .....	34
5.1.1	Far Field Boundary Calculation .....	34
5.1.2	Test laboratory .....	34
5.1.3	Correlation Of Measurements And Simulation .....	35
5.1.4	Estimating conducted power level .....	37
5.2	Simulating a Canonical Antenna Design.....	38
<b>6</b>	<b>Summary</b> .....	<b>41</b>



## List of Figures

Figure 1 – Intel 11000D2W module system block diagram .....	8
Figure 2 – Near field worst case terminology and orientation .....	13
Figure 3– Active antenna inside the platform .....	17
Figure 4 - Closest distance from user to antenna .....	18
Figure 5 – Elevation and azimuth angles .....	20
Figure 6 – Channel 1 upper bound, Spot Absolute Power Density mesh on platform edge at 100% duty cycle	21
Figure 7 – Channel 2 upper bound, Spot Absolute Power Density mesh on platform edge at 100% duty cycle	21
Figure 8 – Channel 3 upper bound, Spot Absolute Power Density mesh on platform edge at 100% duty cycle	22
Figure 9 – Channel 1 Worst case, Spot Absolute Power Density mesh on platform edge at 100% duty cycle	25
Figure 10 – Channel 2 Worst case, Spot Absolute Power Density mesh on platform edge at 100% duty cycle	25
Figure 11 – Channel 3 Worst case, Spot Absolute Power Density mesh on platform edge at 100% duty cycle	26
Figure 12 - One dimensional plots of the power density on Channel 1 .....	27
Figure 13 - One dimensional plots of the power density on Channel 2 .....	27
Figure 14 - One dimensional plots of the power density on Channel 3 .....	28
Figure 15 – Channel 1 Worst case - Integrated power over 1cm <sup>2</sup> on platform edge at 100% duty cycle	29
Figure 16 – Channel 2 Worst case - Integrated power over 1cm <sup>2</sup> an platform edge at 100% duty cycle	29
Figure 17 – Channel 3 Worst case - Integrated power over 1cm <sup>2</sup> an platform edge at 100% duty cycle	30
Figure 18 – HFSS Simulation results in Ch1 .....	31
Figure 19 – HFSS Simulation results in Ch2 .....	32
Figure 20 – HFSS Simulation results in Ch3 .....	32
Figure 21 - Comparison of EIRP simulation to lab measurements – channel 1 .....	35
Figure 22 - Comparison of EIRP simulation to lab measurements – channel 2 .....	35
Figure 23 - Comparison of EIRP simulation to lab measurements – channel 3 .....	36
Figure 24 - Estimate conducted power from EIRP data.....	37
Figure 25 - Simulation of a single Patch antenna .....	38
Figure 26 – Patch Antenna Gain .....	38
Figure 27 – Simulation 3D structure .....	39
Figure 28– Power Density of Canonical Patch Antenna .....	40

## List of Tables

Table 1 – Acronyms	5
Table 2 - Phases configurations for the worst case .....	23
Table 3 – Ratios between Z-power density and total power density .....	24
Table 4 –Base plane integrated power density at zero distance .....	33
Table 5 – Gain calculation from power density per several distances.....	39
Table 6 – Summary of simulation results for RF exposure compliance .....	41



Table 1 – Acronyms

ABS	Acrylonitrile butadiene styrene – the plastic type from which the HP model HSTNN-I22C is built
Ant	Antenna
Az	Azimuth
BB	Base Band
BF	Beam Forming
BT	Bluetooth
BW	Band Width
CAD	Computer Aided Design
CPU	Central Processing Unit
EIRP	Equivalent Isotropic Radiated Power
EI	Elevation
EM	Electro-Magnetic
GHz	Giga Hertz ( $10^9$ Hz)
IF	Intermediate Frequency
MAC	Media Access Control
mmWave	MilliMeter Wave
OTP	One Time Programmable memory
PC	Personal Computer
R&D	Research and Development
RF	Radio Frequency
RFEM	Radio Front End Module
RFIC	Radio Frequency Integrated Circuit
RX	Receive
SKU	Stock Keeping Unit, specific product model version
TPC	Transmit Power Control



T/R SW	Transmit / Receive Switch
TX	Transmit
WiGig	Wireless Gigabit Alliance - the alliance that promoted the 60GHz into 802.11ad standard.



# 1 Document Scope

---

This report is submitted to support the compliance to FCC rule parts §2.1093 and §15.255(g), of Intel 11000D2W WiGig module (FCC ID: PD911000D2), including an active antenna array, embedded inside the Lenovo Model TP00082A platform.

Please note, Lenovo model TP00082A is the regulatory model number. This identical host is also marketed under the name Lenovo X1 tablet. In the report we refer only to TP00082A model.

Per the location of the active antenna array (a.k.a. RFEM) in the Lenovo model TP00082A platform, the distance between the antenna array to the body of an end user, at the closest contact point, will be in the near field. At this time power density measurements are not possible.

Therefore, to obtain an estimation of the near field power density results, we used an EM simulation that includes the RFEM 2 transmitter model, embedded inside the Lenovo model TP00082A. The simulation method and the simulation results are described in this document.

Due to the lack of standardized code validation, benchmarking and uncertainty of the simulation software, the near field to far field results are included for the purpose of providing confidence for the software simulation model used and that the results produced were within an acceptable range when compared with the measured results. The error margins of all test results have been considered collectively by the FCC to determine compliance.

To prove the validity of these results, this report shows how the results of the same simulation are correlated to lab measurements for transition field to far field distances.

The 2<sup>nd</sup> chapter provides relevant background on Intel 11000D2W module. The 3<sup>rd</sup> chapter describes the simulation methodology to determine RF exposure (power density) levels. The 4<sup>th</sup> chapter includes simulation results, and 5<sup>th</sup> chapter the correlation between simulation and lab measurements in near to far field. Chapter 6 summarizes the RF-Exposure analysis.

Please note that this document covers non confidential parts, relevant details and explanations that qualify for confidentiality are included separately in the Operational Descriptions document/exhibit; therefore, not included in the this reports.

## 2 Background – WiGig System Operation

---

### 2.1 System Block Diagram

Intel 11000D2W module is a solution for WiGig connectivity for various platforms. Intel 11000D2W module can be embedded in conventional clamshell PC as well, modern 2 in 1 platforms (detachable platforms) and tablet like platforms (as Lenovo model TP00082A).

Intel 11000D2W WiGig module solution is made of a soldered down module connected to an RFEM using one IF coaxial cable.

Soldered down module: a WiGig BB chip, which implements the WiGig MAC, Modem, BF algorithm, and active antenna array module control, as well as the BB + IF stage circuitry.

RFEM 2: an active antenna array module, which converts between the IF signal and 60GHz signal. It also performs the beam forming functionality by phase shifting the RF signal that goes to each antenna. The RFEM 2 is slave to the WiGig BB chip – all module control and algorithms run on the BB chip.

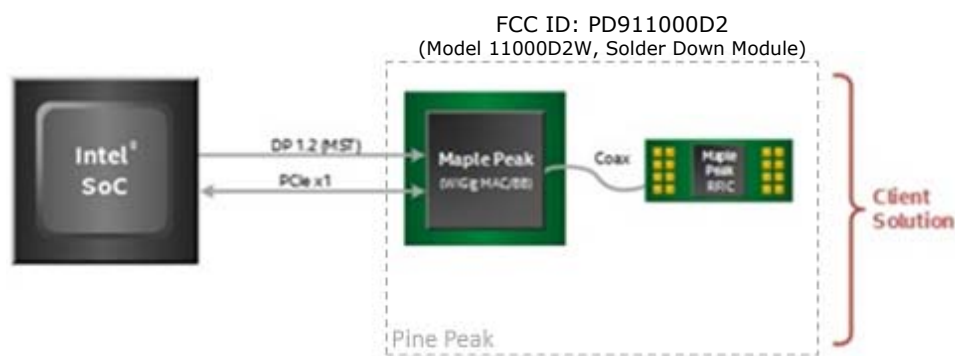


Figure 1 – Intel 11000D2W module system block diagram

In typical application the RFEM is located at the top of the lid of the platform, in order to improve the RF propagation of the communication link.

Note: Also known as Intel internal project code name “Pine Peak” the above described WiGig solder down module solution use the “Maple Peak” Intel chipset (both MAC/BB chip and Radio chip).

### 2.2 Beam Forming

Achieving high bandwidth communication over 60GHz channels usually requires directional antenna at the transmitter and receiver sides. In consumer electronics, fixed directional or mechanically rotated antenna are not practical and electronically steerable antenna are usually used.

In Intel 11000D2W module, such electronic steerable antenna array is being used. Beam forming protocol (defined in the IEEE 802.11ad standard) is used to find the right direction for setting both the RX and TX antenna directions.

Due to the RFEM structure it is not easy to predict the direction and beam forming combination that yields the maximum energy in near field. To find this value a search over the possible beam forming combination was made and the worst case value was taken. Detailed explanation of this process can be found in section 3.4.





## 2.3 TX Duty Cycle

The WiGig protocol, as defined in IEEE 802.11ad, is packet based with time division multiplexing (TDM). Intel 11000D2W module is configured to guarantee that the TX-Duty-Cycle, defined as the ratio of the duration of all transmissions to the total time, is at most 70% over any 10 seconds period. This was established by worst case analysis, as derived from full system simulation, and verified by measurements.

The limited TX-Duty-Cycle is established based on HW and FW implementation with ~100 ms (102.4 ms) measurement duration and 10 seconds averaging. The 70% duty cycle limitation is guaranteed independent of user activity, and therefore it adheres to the source-based time-averaging definition in 2.1093(d)(5).

In addition, the Intel module implementation was measured to obtain maximal TX-Duty-Cycle in a fully loaded system, resulting in a maximum TX-Duty-Cycle of 58% over any 10 seconds period, lower than the upper bound derived from the analysis in this section.

## 2.4 Intel 11000D2W Module In Lenovo Model TP00082A

Intel produces several HW SKUs (variations) of Intel 11000D2W module, which target different types of customer platform products.

Lenovo uses Intel 11000D2W module inside the Lenovo Model TP00082A platform. This SKU is characterized by:

1. supporting channels **1+2+3**
2. Reduced power emission, which translates to:
  - a. Maximum transmit conducted power of **3.0 dBm** aggregated conducted power at the antenna ports.
  - b. Maximum TX duty-cycle of **70%**.



## 3 Simulation Methodology

---

### 3.1 Assessment Considerations

During the system operation mode it is challenging to define a practical system worst case scenario in which the user is exposed to the highest emission level. To ensure coverage of the highest emission the analysis of the worst case corner condition is used and is emphasized in the following:

1. Platform orientation with respect to human body – in most of the cases when the platform is very close to the human body and the energy is directed to the human body, the human body will attenuate the signal. In this case a reliable link can't be achieved, when a reliable link can't be maintained the system enters search mode. In search mode the system will transmit a low duty cycle of less than 1%. This search mode contains signals (of less than 1 ms duration) which happen every 100ms at the maximum output power (3.0dBm for Lenovo TP00082A platform).  
However – in the analysis done in this document system is simulated in operational mode (not in search mode) operating at 70% duty cycle which is much higher than the search mode.
2. Energy direction, beam forming – In order to avoid human body attenuation or object blockage of a reliable link the system beam forming will automatically search for a path that will establish a more reliable link. So, in real life, in most of the cases the EM path will not be directed towards the human body.  
However – in the analysis presented in this document worst case beam forming direction is used.

Please note; the above worst case assessment description is very conservative in that it is very unlikely this case would happen under normal usage conditions. Since we cannot state with 100% certainty that this is impossible we kept this worst case assessment methodology, we ask that this is taken into consideration.

### 3.2 Establishing worst case near-field test configuration

Finding the worst case emission in near field across platform boundary requires searching on two orthogonal domains. One domain is the location – need to find the place that has the worst case energy. The other domain that has to be searched is the antenna phases – need to search over the various antenna phases and find the antenna phase combination that gives the worst case value. Section 3.4 below explains how these two domains are investigated.

After the completion of the worst case phase analysis, the phases found during this analysis are used to find the worst case integrated energy across all1cm<sup>2</sup>. EM simulation is used for this analysis.

Transition to far field analysis is both simulated and correlated against measured lab results.

### 3.3 Simulation tool

#### 3.3.1 Tool description

For the EM simulation the commercially available ANSYS HFSS tool version 2014 is used. The ANSYS HFSS tool is used in industry for simulating 3-D full-wave electromagnetic fields. Intel uses this EM simulation tool due to its' gold-standard accuracy, advanced solver and high-performance computing technology capabilities for doing accurate and rapid design of high-frequency components.

#### 3.3.2 Solver description

The HFSS simulation is done using the Finite Element Method which operates in the frequency domain. The HFSS is based on an accurate direct solver with first order basis functions.

---



### 3.3.3 Convergence criteria and Power Density Calculations

The HFSS uses volume air box containing the simulated area to calculate the EM fields. The box is truncated by PML (Perfect Match Layer) boundary condition. The simulation uses adaptive mesh technique to meet the exit criteria of  $\Delta S < 0.02$ . The  $\Delta S$  is the change in the magnitude of the S-parameters between two consecutive passes, if the magnitude and phase of all S-parameters change by an amount less than the Maximum  $\Delta S$  per Pass value from one iteration to the next, the adaptive analysis stops.

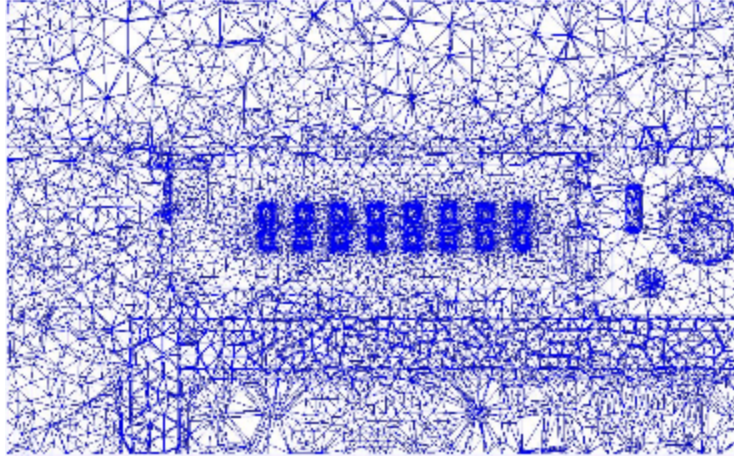


Illustration of the Adaptive Mesh Technique

After having the simulated electrical and magnetic (E & H) fields in each point in the mesh, the Poynting vector is calculated. The integrated power density on a given surface is calculated as the surface integral of the Poynting vector:

$$W = \frac{1}{2} \text{Re} \int_S (\vec{E} \times \vec{H}^*) \cdot \vec{n} dS$$

### 3.4 Finding near field worst case simulation configuration

As explained previously near field analysis requires finding worst case location (along the searched planes) and antenna phase values. As further explained the search should be done on two domains:

- 1) Look for the worst case position (across the search plane).
- 2) Look for the worst case antenna phases

Note: the search plane here is defined as the plane that is used for the calculation of the worst case antenna phase values. This is the x-y plane that is adjacent to the platform (tablet) outer plastic (at the location of the RFEM) and represent the worst case scenario where the user is the closest to the platform:



Search Plane is the x-y plane (i.e. the transparent plane as illustrated in this picture)

### 3.4.1 Terminology:

- Element – each one of the radiating elements that are used in the system (the antenna array has 16 radiating elements). We denote the antenna element with index  $\mathbf{k}$  in this explanation.
- $\mathbf{N}$  – number of chains in the RFEM,  $\mathbf{N}=16$ .
- Point – each point on the grid that is used for searching for the worst case position. The points are spaced 0.1mm from each other. The grid point would be denoted as  $\mathbf{g}$  in this explanation.
- Complex E field vector generated by the  $k^{\text{th}}$  antenna element at point  $\mathbf{g}$  :
- Complex H field vector generated by the  $k^{\text{th}}$  antenna element at point  $\mathbf{g}$  :

$$\vec{E}_{k,g} = \hat{x}(\text{Re}[E_{kx,g}] + j\text{Im}[E_{kx,g}]) + \hat{y}(\text{Re}[E_{ky,g}] + j\text{Im}[E_{ky,g}]) + \hat{z}(\text{Re}[E_{kz,g}] + j\text{Im}[E_{kz,g}])$$

$$\vec{H}_{k,g} = \hat{x}(\text{Re}[H_{kx,g}] + j\text{Im}[H_{kx,g}]) + \hat{y}(\text{Re}[H_{ky,g}] + j\text{Im}[H_{ky,g}]) + \hat{z}(\text{Re}[H_{kz,g}] + j\text{Im}[H_{kz,g}])$$

- $\hat{x}$ ,  $\hat{y}$ ,  $\hat{z}$  – are unit direction vectors having unit magnitude and are mutually orthogonal to each other.
- Without loss of generality in this explanation RFEM and search plane are in the  $\hat{x}$ ,  $\hat{y}$  plane and the integrated  $1\text{cm}^2$  plane is perpendicular to  $\hat{z}$  direction.

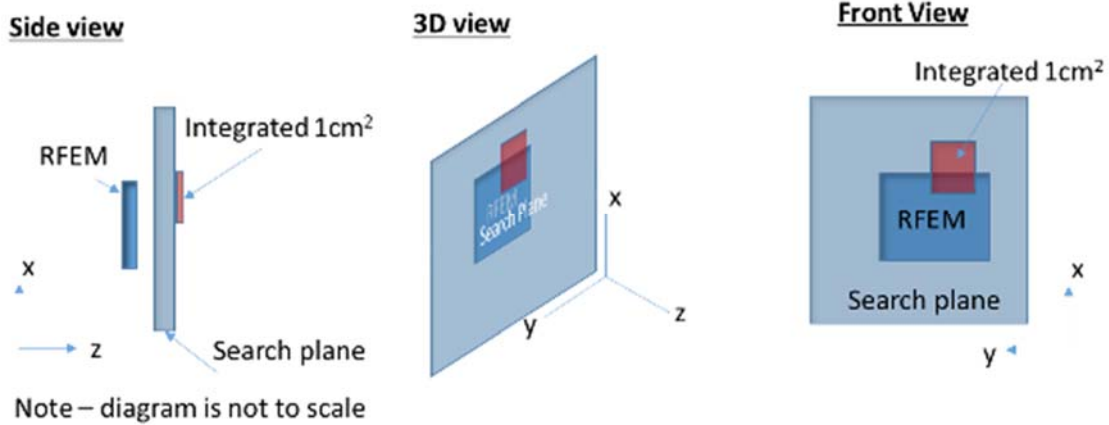


Figure 2 – Near field worst case terminology and orientation

### 3.4.2 Primer on field vector representation:

$E$  and  $H$  fields generated by  $k$  the chain are:

$$\vec{E}_k = \vec{x}(\text{Re}[E_{kx}] + j\text{Im}[E_{kx}]) + \vec{y}(\text{Re}[E_{ky}] + j\text{Im}[E_{ky}]) + \vec{z}(\text{Re}[E_{kz}] + j\text{Im}[E_{kz}])$$

$$\vec{H}_k = \vec{x}(\text{Re}[H_{kx}] + j\text{Im}[H_{kx}]) + \vec{y}(\text{Re}[H_{ky}] + j\text{Im}[H_{ky}]) + \vec{z}(\text{Re}[H_{kz}] + j\text{Im}[H_{kz}])$$

$E$  and  $H$  fields generated by all  $N$  chains are

$$\vec{E}_{\text{All}} = \vec{x} \sum_{k=1}^N (\text{Re}[E_{kx}] + j\text{Im}[E_{kx}]) + \vec{y} \sum_{k=1}^N (\text{Re}[E_{ky}] + j\text{Im}[E_{ky}]) + \vec{z} \sum_{k=1}^N (\text{Re}[E_{kz}] + j\text{Im}[E_{kz}])$$

$$\vec{H}_{\text{All}} = \vec{x} \sum_{k=1}^N (\text{Re}[H_{kx}] + j\text{Im}[H_{kx}]) + \vec{y} \sum_{k=1}^N (\text{Re}[H_{ky}] + j\text{Im}[H_{ky}]) + \vec{z} \sum_{k=1}^N (\text{Re}[H_{kz}] + j\text{Im}[H_{kz}])$$

Poynting vector generated by all  $N$  chains is

$$\begin{aligned}
 \overrightarrow{P_{\text{General,All}}} &= \frac{1}{2} \overrightarrow{E_{\text{All}}} \times \overrightarrow{H_{\text{All}}}^* \\
 &= \frac{1}{2} \langle \vec{x} \left\{ \sum_{k=1}^N (\text{Re}[E_{ky}] + j\text{Im}[E_{ky}]) \sum_{k=1}^N (\text{Re}[H_{kz}] - j\text{Im}[H_{kz}]) \right. \\
 &\quad \left. - \sum_{k=1}^N (\text{Re}[E_{kz}] + j\text{Im}[E_{kz}]) \sum_{k=1}^N (\text{Re}[H_{ky}] - j\text{Im}[H_{ky}]) \right\} \\
 &\quad + \vec{y} \left\{ \sum_{k=1}^N (\text{Re}[E_{kz}] + j\text{Im}[E_{kz}]) \sum_{k=1}^N (\text{Re}[H_{kx}] - j\text{Im}[H_{kx}]) \right. \\
 &\quad \left. - \sum_{k=1}^N (\text{Re}[E_{kx}] + j\text{Im}[E_{kx}]) \sum_{k=1}^N (\text{Re}[H_{kz}] - j\text{Im}[H_{kz}]) \right\} \\
 &\quad + \vec{z} \left\{ \sum_{k=1}^N (\text{Re}[E_{kx}] + j\text{Im}[E_{kx}]) \sum_{k=1}^N (\text{Re}[H_{ky}] - j\text{Im}[H_{ky}]) \right. \\
 &\quad \left. - \sum_{k=1}^N (\text{Re}[E_{ky}] + j\text{Im}[E_{ky}]) \sum_{k=1}^N (\text{Re}[H_{kx}] - j\text{Im}[H_{kx}]) \right\} \rangle
 \end{aligned}$$

Power flow is

$$\begin{aligned}
 \text{Re}[\overrightarrow{P_{\text{General,All}}}] &= \frac{1}{2} \langle \vec{x} \left\{ \sum_{k=1}^N \text{Re}[E_{ky}] \sum_{k=1}^N \text{Re}[H_{kz}] + \sum_{k=1}^N \text{Im}[E_{ky}] \sum_{k=1}^N \text{Im}[H_{kz}] - \sum_{k=1}^N \text{Re}[E_{kz}] \sum_{k=1}^N \text{Re}[H_{ky}] \right. \\
 &\quad \left. - \sum_{k=1}^N \text{Im}[E_{kz}] \sum_{k=1}^N \text{Im}[H_{ky}] \right\} \\
 &\quad + \vec{y} \left\{ \sum_{k=1}^N \text{Re}[E_{kz}] \sum_{k=1}^N \text{Re}[H_{kx}] + \sum_{k=1}^N \text{Im}[E_{kz}] \sum_{k=1}^N \text{Im}[H_{kx}] - \sum_{k=1}^N \text{Re}[E_{kx}] \sum_{k=1}^N \text{Re}[H_{kz}] \right. \\
 &\quad \left. - \sum_{k=1}^N \text{Im}[E_{kx}] \sum_{k=1}^N \text{Im}[H_{kz}] \right\} \\
 &\quad + \vec{z} \left\{ \sum_{k=1}^N \text{Re}[E_{kx}] \sum_{k=1}^N \text{Re}[H_{ky}] + \sum_{k=1}^N \text{Im}[E_{kx}] \sum_{k=1}^N \text{Im}[H_{ky}] - \sum_{k=1}^N \text{Re}[E_{ky}] \sum_{k=1}^N \text{Re}[H_{kx}] \right. \\
 &\quad \left. - \sum_{k=1}^N \text{Im}[E_{ky}] \sum_{k=1}^N \text{Im}[H_{kx}] \right\} \rangle
 \end{aligned}$$

Power flow to  $Z$  is

$$\begin{aligned}
 \vec{z} \cdot \text{Re}[\overrightarrow{P_{\text{General,All}}}] &= \frac{1}{2} \langle \left\{ \sum_{k=1}^N \text{Re}[E_{kx}] \sum_{k=1}^N \text{Re}[H_{ky}] + \sum_{k=1}^N \text{Im}[E_{kx}] \sum_{k=1}^N \text{Im}[H_{ky}] - \sum_{k=1}^N \text{Re}[E_{ky}] \sum_{k=1}^N \text{Re}[H_{kx}] \right. \\
 &\quad \left. - \sum_{k=1}^N \text{Im}[E_{ky}] \sum_{k=1}^N \text{Im}[H_{kx}] \right\} \rangle
 \end{aligned}$$



### 3.4.3 Domain search for worst case direction

The two domain search is completed as follows:

- A. First find a direction (location) for the worst case 1cm<sup>2</sup> square using upper bound methods. The basic concept behind the upper bound method is to assume that there could be an “ideal beam forming” mechanism that could align the phases of all the elements for both E and H field (obviously in real life this cannot happen – this is the reason that this is an upper bound method). When this ideal mechanism is used then all the complex phasors are aligned to the same phase, hence the phasor absolute value can be used instead of the phasor -> the E (and H) field for any direction is the sum of the magnitude of the fields (look at section 3 below for more formal description). This method provides the worst case position independent of the antenna phases -> it allows finding the worst case location with this “ideal beam forming” mechanism. Item 3 below translate the above verbal description to more formal mathematical wording.
- B. After the worst case direction is found using the upper bound method, the antenna phases are aligned to this direction. The antenna phases are aligned to maximize the power across the 1cm<sup>2</sup> that was found using the upper bound method. The method that is used to find the required antenna phases is: first order the antenna according to the power contribution on the found 1cm<sup>2</sup> from the highest to the lowest. Then start by activating the antenna that contribute the most and set its phase to 0, then activate the 2<sup>nd</sup> antenna and search over the phases for the 2<sup>nd</sup> antenna. Choose the phase that maximize the power of the two antenna elements. For finding the phase for the third antenna fix antenna 1 phase to zero and the 2<sup>nd</sup> antenna to the value that was found before – now search for the phases for the third antenna phases that maximize the power. Continue with the same process till the 16<sup>th</sup> element.
- C. Calculate the power density with the antenna phases that were found in the previous section (section b).

The above process can be written as the following algorithm:

1. A grid is defined with 0.1mm spacing.
2. At each point in the grid, the complex E & H fields are calculated using each one of the 16 radiating elements separately. Each one of the calculated E & H fields are 3D complex vectors, so the simulation output from this stage is 16 3D complex E field vectors & 16 3D complex H field vectors. The vectors are defined as:  

$$\vec{E}_{k,g} = \hat{x}(\text{Re}[E_{kx,g}] + j\text{Im}[E_{kx,g}]) + \hat{y}(\text{Re}[E_{ky,g}] + j\text{Im}[E_{ky,g}]) + \hat{z}(\text{Re}[E_{kz,g}] + j\text{Im}[E_{kz,g}])$$

$$\vec{H}_{k,g} = \hat{x}(\text{Re}[H_{kx,g}] + j\text{Im}[H_{kx,g}]) + \hat{y}(\text{Re}[H_{ky,g}] + j\text{Im}[H_{ky,g}]) + \hat{z}(\text{Re}[H_{kz,g}] + j\text{Im}[H_{kz,g}])$$
3. Upper bound assumption is used to derive the E & H field on each one of the grid point, the following sections describes the upper bound method that is used:

- a. The calculation is made separately for E field and H field.
- b. For E field the following calculation is made independently for each one of the grid point:

$$\vec{E}_{UB,g} = \hat{x} \sum_{k=1}^N \sqrt{\text{Re}[E_{kx,g}]^2 + \text{Im}[E_{kx,g}]^2} + \hat{y} \sum_{k=1}^N \sqrt{\text{Re}[E_{ky,g}]^2 + \text{Im}[E_{ky,g}]^2} + \hat{z} \sum_{k=1}^N \sqrt{\text{Re}[E_{kz,g}]^2 + \text{Im}[E_{kz,g}]^2} = \hat{x} \sum_{k=1}^N |E_{kx}| + \hat{y} \sum_{k=1}^N |E_{ky,g}| + \hat{z} \sum_{k=1}^N |E_{kz,g}|$$

The magnitude of the complex E vector is summed over the antenna elements. The summation is being done for each one of the grid point and for each one for each direction independently.



- c. The output of the previous section is 3D real vector of the E field on each one of the simulated grid points in each direction. The physical implementation is that an ideal beam forming was done for the E field for each one of the points.
- d. Same process as described in section b is being done for the H field.

$$\begin{aligned} \vec{H}_{UB,g} = \hat{x} \sum_{k=1}^N \sqrt{\text{Re}[H_{kx,g}]^2 + \text{Im}[H_{kx,g}]^2} + \hat{y} \sum_{k=1}^N \sqrt{\text{Re}[H_{ky,g}]^2 + \text{Im}[H_{ky,g}]^2} \\ + \hat{z} \sum_{k=1}^N \sqrt{\text{Re}[H_{kz,g}]^2 + \text{Im}[H_{kz,g}]^2} = \hat{x} \sum_{k=1}^N |H_{kx,g}| + \hat{y} \sum_{k=1}^N |H_{ky,g}| + \hat{z} \sum_{k=1}^N |H_{kz,g}| \end{aligned}$$

- e. In each point in the grid the poynting vector is calculated by vector multiplication of E & H field which are added-up in section b & d. As explained before, without loss of generality we assume that the search plane is X/Y plane and the energy propagate to Z dimension, this translates to:

$$\begin{aligned} P_{g,z} &= \frac{1}{2} \text{Re}\{\hat{z} \cdot (\vec{E} \times \vec{H}^*)\} = \frac{1}{2} \text{Re}\{\hat{z} \cdot ((\dots)\hat{x} + (\dots)\hat{y} + (E_x H_y^* - E_y H_x^*)\hat{z})\} = \\ &= \frac{1}{2} \text{Re}\{E_x H_y^* - E_y H_x^*\} \leq \frac{1}{2} |E_x H_y^* - E_y H_x^*| \leq \\ &\leq \frac{1}{2} |E_x H_y^*| + \frac{1}{2} |E_y H_x^*| = \frac{1}{2} \{|E_x| \cdot |H_y| + |E_y| \cdot |H_x|\} = \\ P_{UpperBound,z,g} &= \frac{1}{2} \langle \sum_{i=1}^N |E_{ix}| \sum_{i=1}^N |H_{iy}| + \sum_{i=1}^N |E_{iy}| \sum_{i=1}^N |H_{ix}| \rangle \end{aligned}$$

The final value  $(\frac{1}{2} \langle \sum_{i=1}^N |E_{ix}| \sum_{i=1}^N |H_{iy}| + \sum_{i=1}^N |E_{iy}| \sum_{i=1}^N |H_{ix}| \rangle)$  obtained in each grid point represents an upper bound value i.e. this value is always greater or equal than the real pointing vector magnitude  $(\frac{1}{2} \text{Re}\{\hat{z} \cdot (\vec{E} \times \vec{H}^*)\})$ .

4. The above calculated poynting vectors are used to estimate the power across 1cm<sup>2</sup> area. Note that in this example the relevant direction for the pointing vector is  $\hat{z}$  direction

$$P_{1cm^2} = \iint_{1cm^2} \overline{P_{UpperBound}_{g,x,y,z}} \cdot \hat{z}$$

5. The 1cm<sup>2</sup> area with the highest power value is used as the worst case the direction. The antenna phases are aligned to maximize the energy in this 1cm<sup>2</sup> area as explained below:

- a. Turn on each element one-by-one to find order of power intensity in the 1<sup>^</sup>cm window. (Find the order of contribution)
- b. Sort in the power order from the highest to the lowest #0 to #15.
- c. Turn on #0 with phase P0=0. (reference)
- d. Turn on #1 and change phase to maximize the power and find the phase P1.
- e. Keep P0 and P1, turn on #2 and do same.
- f. Repeat for the rest of the antennas.

6. Using the antenna phases that were calculated in step 6 the power density is calculated along the base plane.





## 3.5 3D Models Used In the Simulation

### 3.5.1 RFEM Housing Inside Intel 1100D2W Module

3D Intel 1100D2W module CAD files are used in the EM simulation to allow correct exposure level simulation.

Please refer to the following picture to see RFEM placement inside the Lenovo Model TP00082A platform.



Figure 3– Active antenna inside the platform

### 3.5.2 Closest Distance To The Body Of An End User

The closest distance between the active antennas to the skin of an end user is when the person holding the unit and touching the plastic (platform surface). At this case the distance between a hand or body to the active antenna is 2.03mm. The Figure 4 is an illustration showing the closest distance between a hand or body to the active antenna, note that Figure 4 is not to scale.

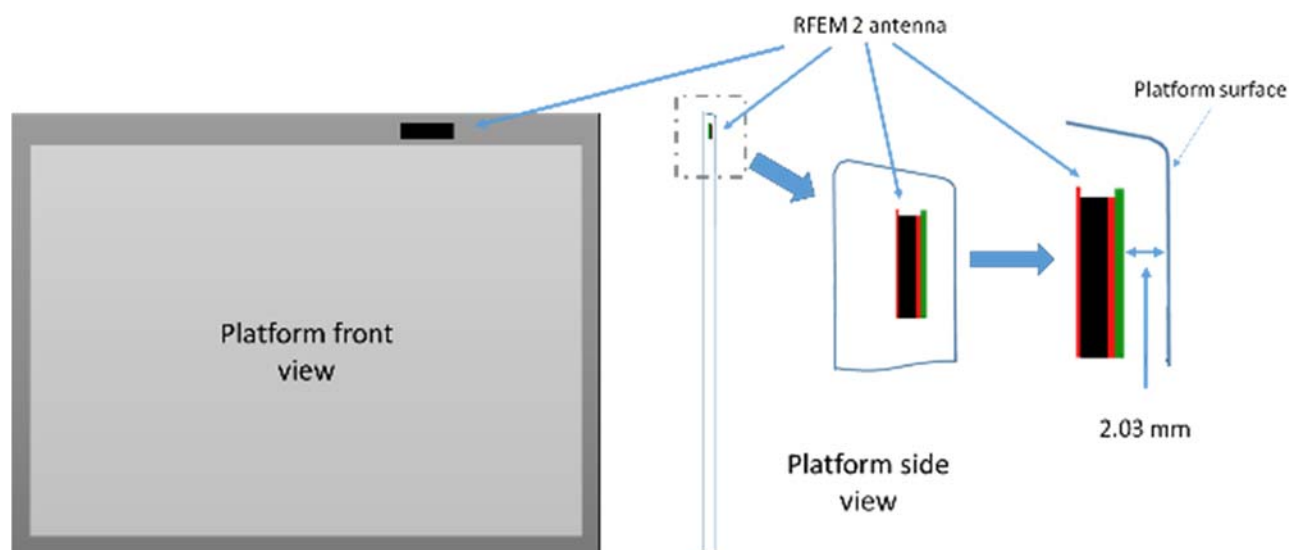


Figure 4 - Closest distance from user to antenna

### 3.5.3 Metals In Proximity Of The RFEM

All the metals that are in the RFEM region (10mm on each side) were included in the simulation. More details on this can be found in the WiGig subsystem theory of operation section 5.3.

### 3.6 Antenna Feed

The EM simulation uses a complete 3D model of the RFEM2 antenna. The model includes the antenna elements as well as their feeding lines.

Both PCBs (antenna PCB and Si PCB) are simulated. The simulation starts at the silicon bumps (the metal bump that is connected to the Silicon and soldered to the board).

In the simulation, the amplitudes are derived for each excitation separately such as the total aggregated conducted output power at the antenna feed points is 3.0 dBm. The feed power to each elements is -9.0 dBm. In addition, the simulation is conducted using 100% TX duty cycle.

Phases are derived for each excitation separately to simulate the worst case condition. Chapter 3.4 explains how the phases are derived to find worst case condition. The total power (same per element) is used to build radiated power through beam forming.

For building the beamforming pattern the same power is used per element, while phase is changed per element, please look at chapter 2.2 for more information about the beamforming.

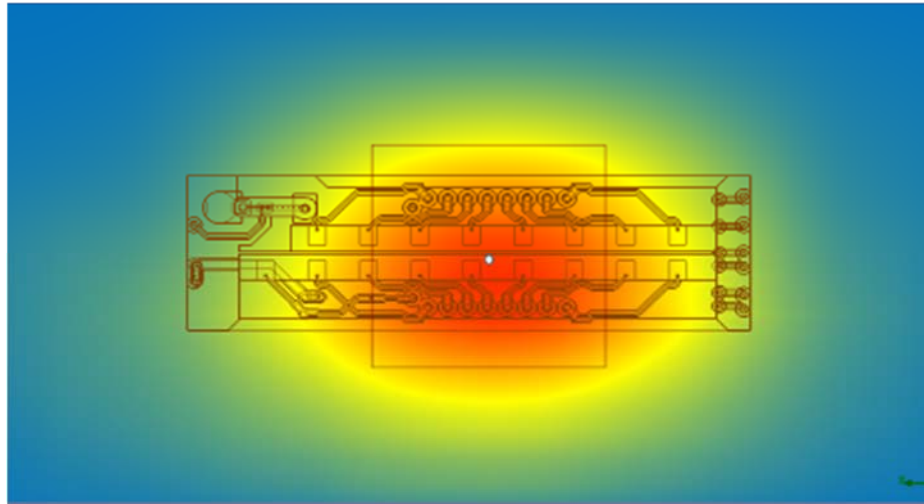


## 4 Simulation Results

---

In the following section, for each channel we'll present the results detail according to the methodology explained in section 3.4:

- Simulation results of the absolute power density for each spot across the Mesh ( $P_{UpperBound_{z,g}}$ ) in z direction and the worst case coordinate. Please note that this value is spot power density and not integrated power density over  $1\text{cm}^2$  (even though  $1\text{mW}/\text{cm}^2$  scale is used, this value represents an upper bound power density for each spot of the mesh which is much smaller area than  $1\text{cm}^2$ ).
- The results of the spot power density in z direction using the antenna phases corresponding to the worst case coordinate found above. In this section correction factors are presented, these factors are the ratios between the spot power density using the z component of Poynting vector and the spot power density using the three components of Poynting vector. These factors are presented in Table 3 of section 4.2.
- One dimensional cut of the mesh spot power density – showing 1 dimensional cut of the mesh power density. The X cut is done with the Y in the maximum value, similarly Y cut is done with the X in the maximum value. These results show the results using the z component of the Poynting vector.
- Integrated power density over  $1\text{cm}^2$  – these figures present the integrated power density across  $1\text{cm}^2$  using the z component of Poynting vector. Each point in the figure represents integration over  $1\text{cm}^2$ , where the point location is the location of the center of the square. As an example in the figure below, the white dot represent the center of the  $1\text{cm}^2$  square.
- The worst case power-density in z direction integrated over  $1\text{cm}^2$  using the worst case antenna phases computed by the simulation versus the distance from the platform boundary and the final value at zero distance obtained by the application of the scaling factors between normal and global Poynting vector components.



### 4.1 Upper bound simulation results

The figures below present upper bound Z spot power density (as described in section 3.4). In each figure the spot power (in  $\text{mW}/\text{cm}^2$ ) is shown as well as the place of this maximum value.

Please note that in the bottom of each figure there is an area with  $\sim 0$  energy, this is explained by the fact that there is metal in this place in the platform and is an expected result.

---

In each one of the figures the worst case 1cm<sup>2</sup> is plotted in the figure, and the co-ordinate of the center of the 1cm<sup>2</sup> is given (0,0 for the co-ordination system is lower left RFEM corner). Please note that since the worse-case conditions are searched over a plane for near field, then the azimuth and the elevation are not relevant. The worst case position is calculated using all the power density spot issued from the upper bound simulation results, even the hotspots on top of the zero power density metallic region (~0 energy area). The upper bound worst case power density condition happens to be at the platform-metal edge as shown in Figure 6, Figure 7 and Figure 8. We leverage the phase conditions (summarized in Table 2) for each antenna element that resulted in these worst case conditions to evaluate final integrated power density. The mathematical basis for using these as the worst case phase conditions to evaluate the final integrated power density is provided in Section 3.4.3.

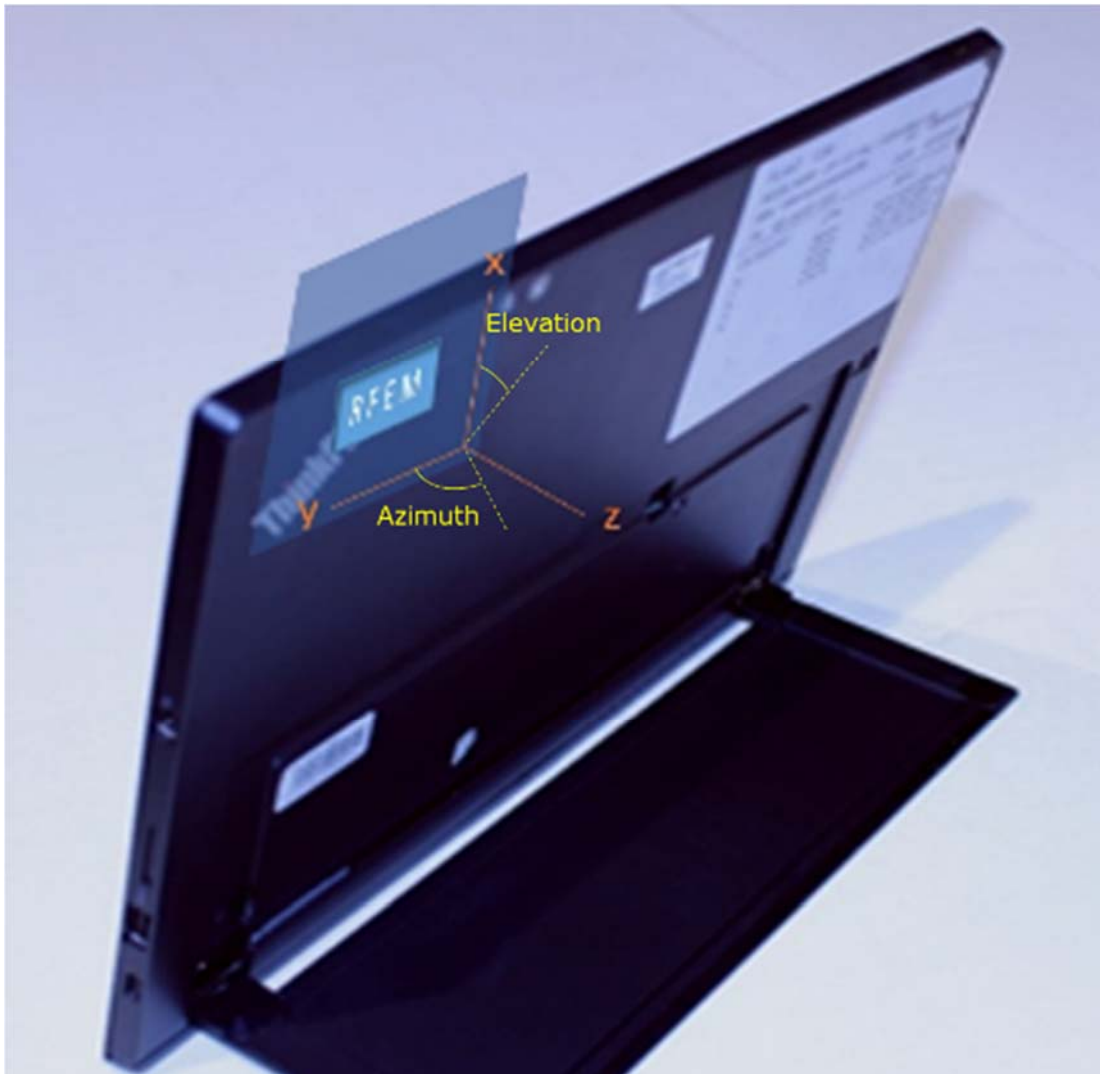


Figure 5 – Elevation and azimuth angles

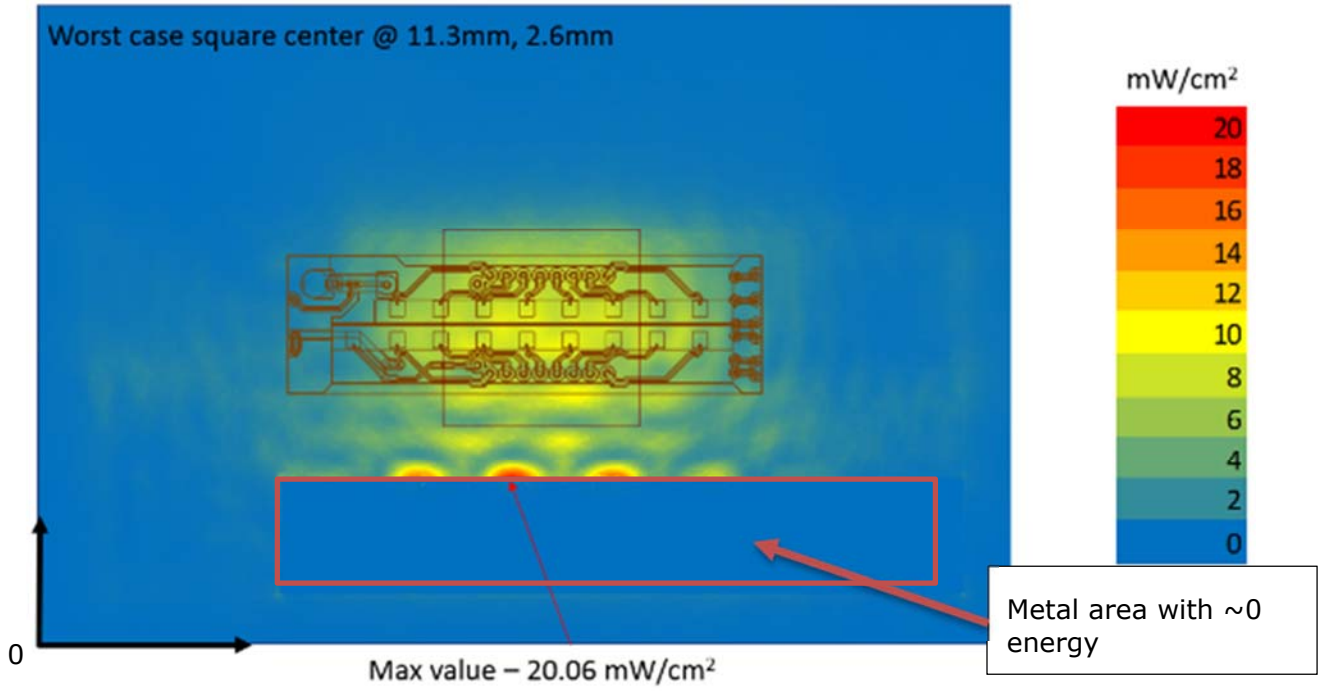


Figure 6 – Channel 1 upper bound, Spot Absolute Power Density mesh on platform edge at 100% duty cycle

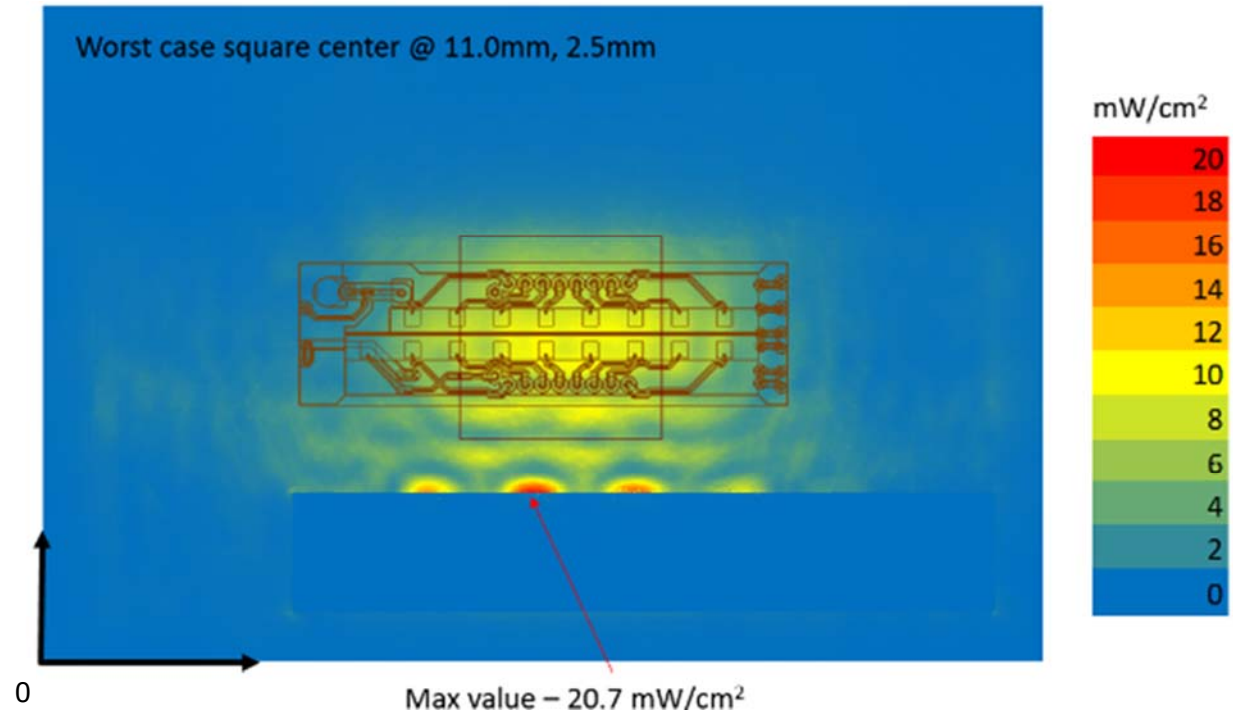


Figure 7 – Channel 2 upper bound, Spot Absolute Power Density mesh on platform edge at 100% duty cycle

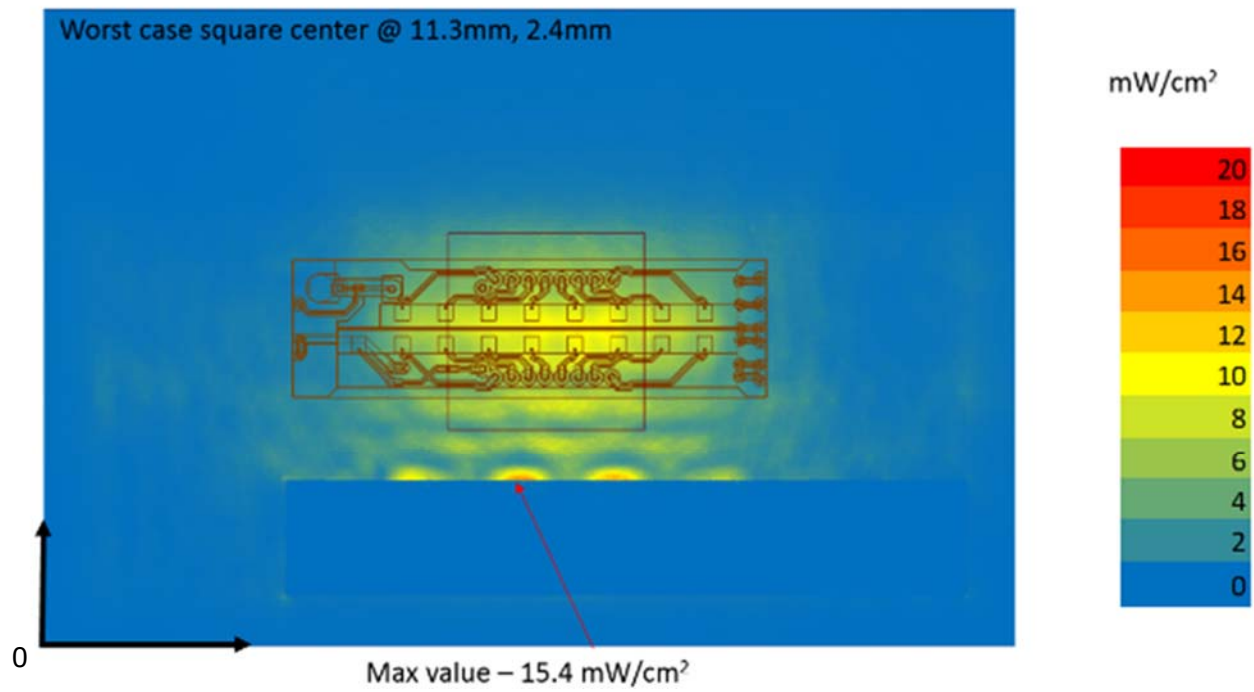


Figure 8 – Channel 3 upper bound, Spot Absolute Power Density mesh on platform edge at 100% duty cycle



## 4.2 Spot power density values with worst antenna phases

The Table 2 shows the phase for each antenna elements per channel for the worst case found as described in the chapter 3.4.

Antenna index	Phases [Degrees]		
	Channel 1	Channel 2	Channel 3
0	0	45	0
1	45	45	0
2	135	135	90
3	315	315	270
4	90	135	135
5	135	180	135
6	225	270	225
7	0	45	315
8	270	270	135
9	270	270	180
10	0	0	270
11	180	180	90
12	315	0	315
13	0	0	315
14	90	90	45
15	225	225	135

**Table 2 - Phases configurations for the worst case**

The amplitude on each antenna as -9dBm as explained in chapter 3.6.

The Figure 9, Figure 10 and Figure 11 present power density in the body direction using worst case antenna phases presented in the Table 2 - Phases configurations for the worst case Table 2. The simulated power density area has a size of 49.5mm x 32.4mm, this area corresponds to the blue delimitation.

Table 3 presents the ratios (linear and logarithmic) at the highest spot value for the Z trajectory between the power density worst case value along the body direction ( $S_z$ ) and the power density worst case value along the propagation direction ( $S_{tot}$ ) for all channels and taking into account all components. This table confirms that the power density component along Z is the principal contributor in the total power density.



	Channel 1	Channel 2	Channel 3
<b>Mag <math>S_{tot}</math> (maximum poynting spot value with all components)</b> [mW/cm <sup>2</sup> ]	3.91	3.346	3.948
<b><math>S_z</math> (trajectory of the above on Z direction)</b> [mW/cm <sup>2</sup> ]	3.781	3.331	3.866
<b>Ratio (<math>S_z / S_{tot}</math>) (linear)</b>	0.97	0.99	0.98
<b>Ratio <math>10\log(S_z / S_{tot})</math> (dB)</b>	-0.15	-0.02	-0.1

**Table 3 – Ratios between Z-power density and total power density**

Please note that in the bottom of each figure there is a zero power density metallic region with  $\sim 0$  energy, this is explained by the fact that there is metal in this place in the platform and is an expected result.



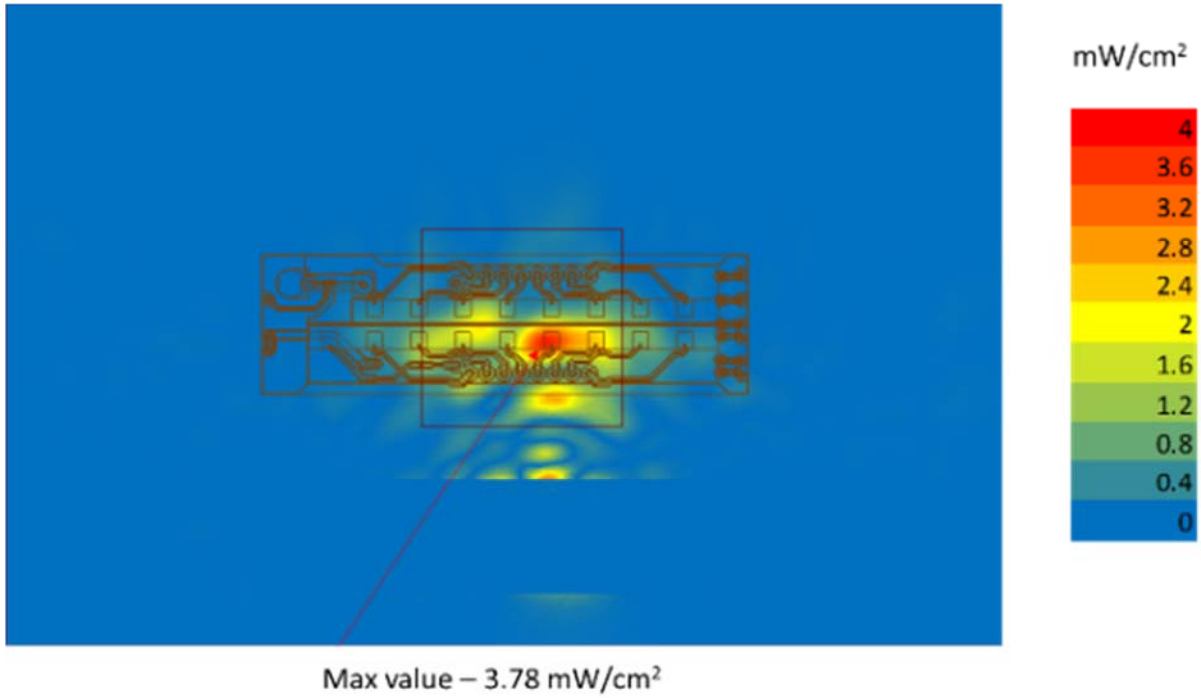


Figure 9 – Channel 1 Worst case, Spot Absolute Power Density mesh on platform edge at 100% duty cycle

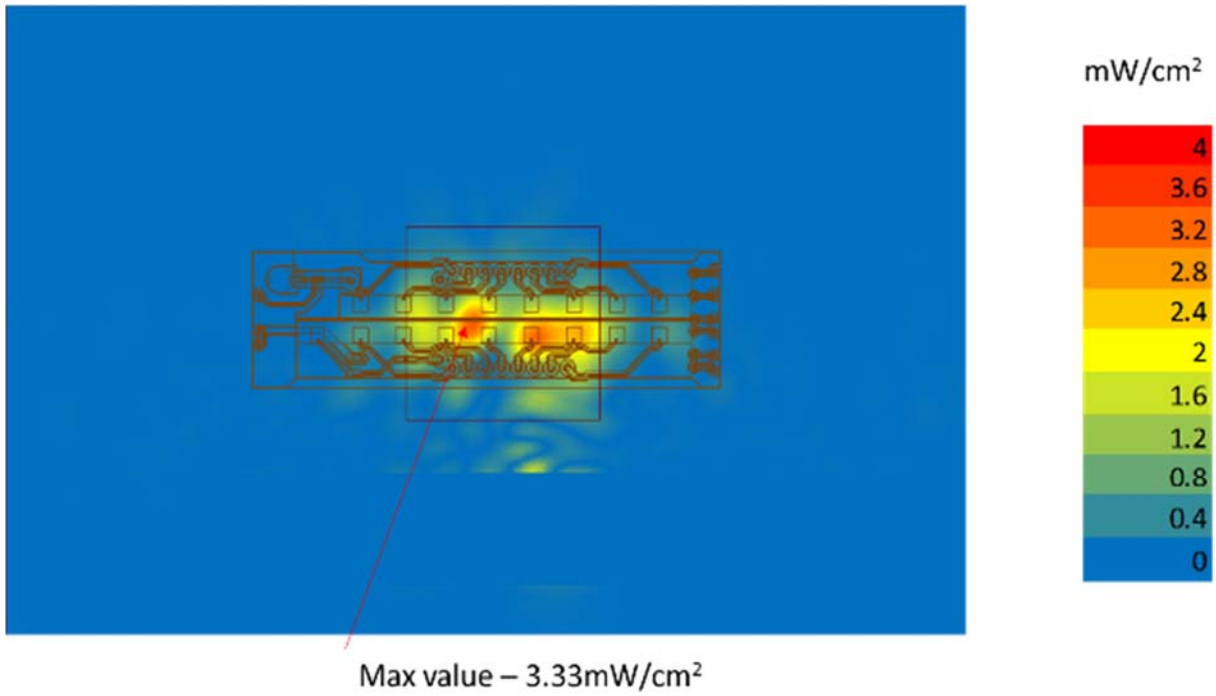


Figure 10 – Channel 2 Worst case, Spot Absolute Power Density mesh on platform edge at 100% duty cycle

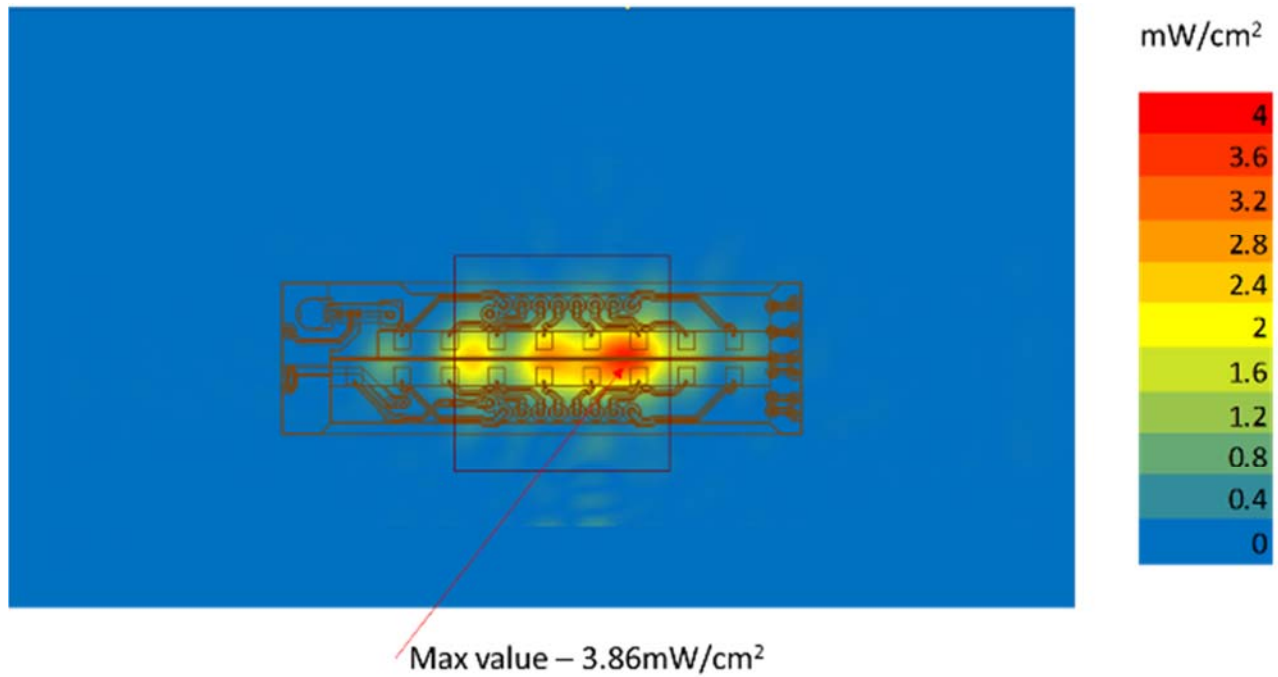


Figure 11 – Channel 3 Worst case, Spot Absolute Power Density mesh on platform edge at 100% duty cycle

The highest value shown in this figure is a point and not yet integrated over the 1cm<sup>2</sup>. The final power density value is given in section 4.4.



### 4.3 One dimensional cut of the mesh spot power density

In Figure 12 - Figure 14 below, we present a subset of the simulation results from the Z-Spot power density values with worst case antenna (Chapter 4.2).

The subset is a 1 dimensional cut in the X axis and Y axis that shows the behavior of the near field power density at zero distance.

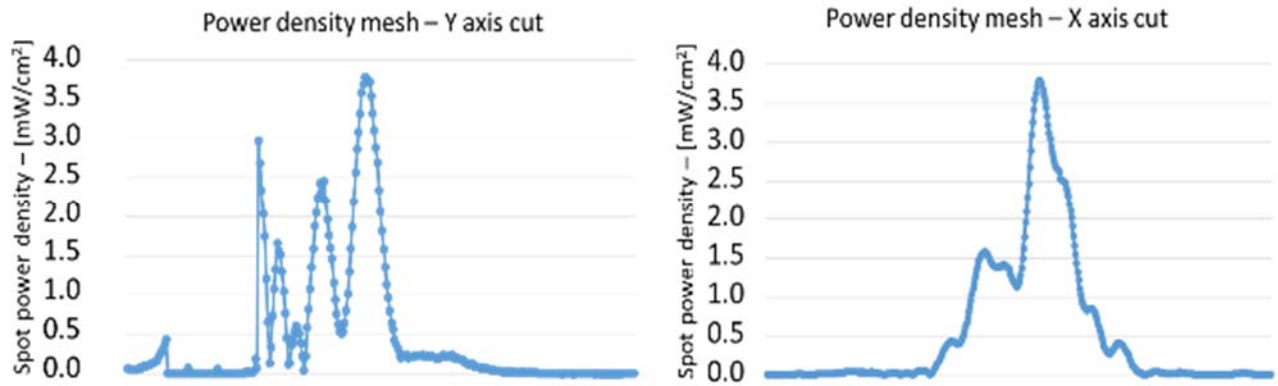


Figure 12 - One dimensional plots of the power density on Channel 1

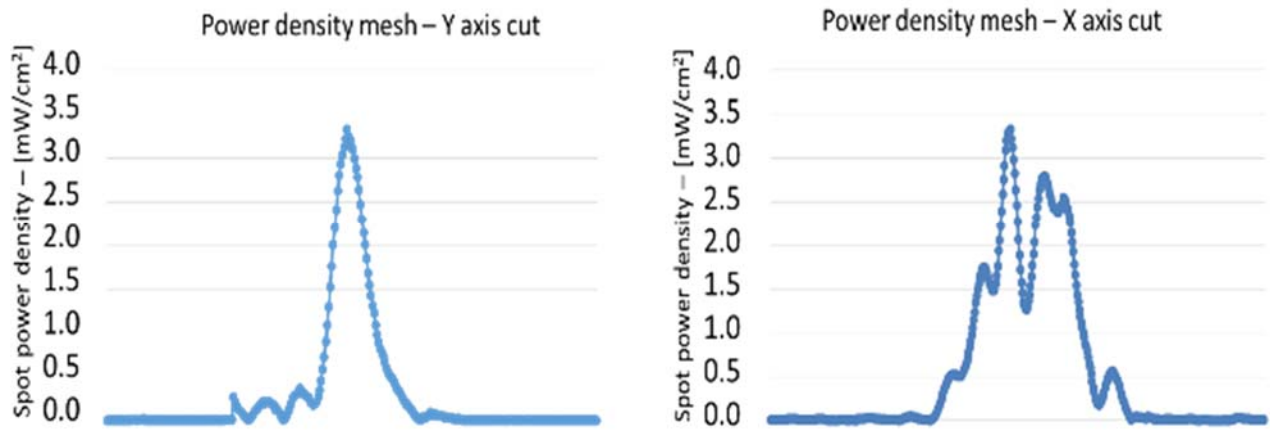


Figure 13 - One dimensional plots of the power density on Channel 2

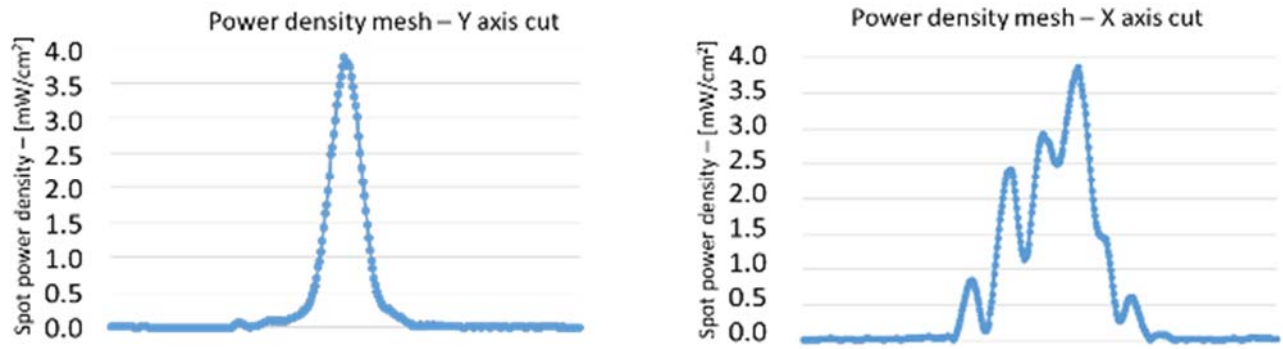


Figure 14 - One dimensional plots of the power density on Channel 3



## 4.4 Integrated power density over 1cm<sup>2</sup>

Figure 15 - Figure 17 below present the Z-integrated power density over 1cm<sup>2</sup>, for the worst case scenario as explained in section 4.1. The power density area has a size of 39.5 mm x 22.4 mm, this area corresponds to the blue area delimitation.

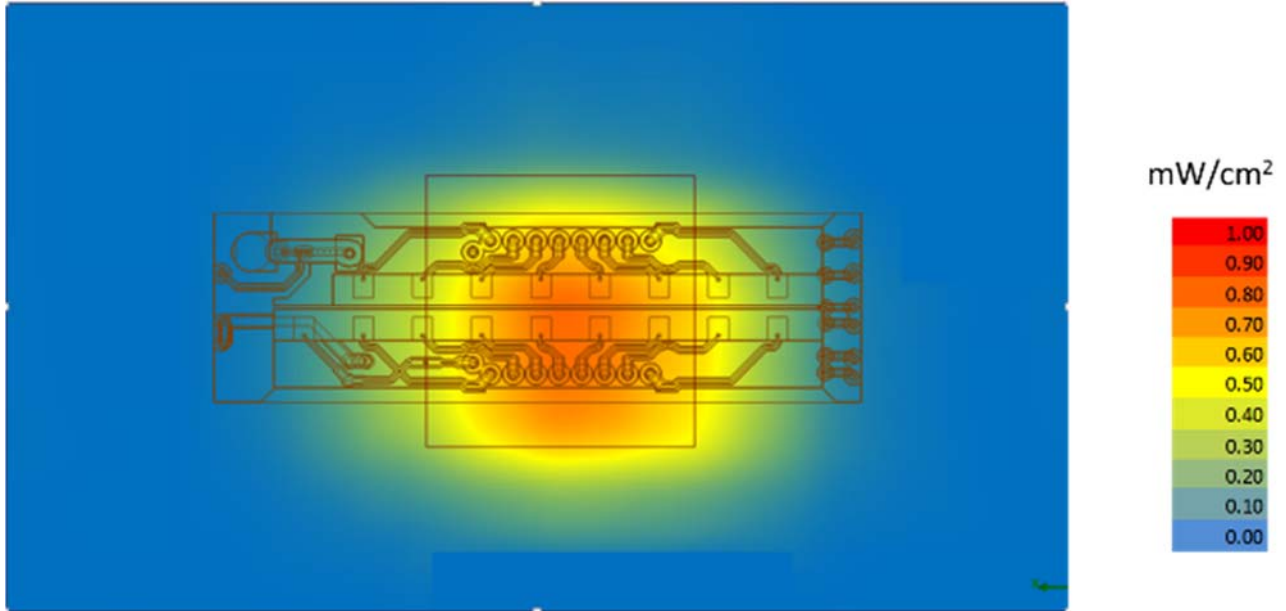


Figure 15 – Channel 1 Worst case – Integrated power over 1cm<sup>2</sup> on platform edge at 100% duty cycle

The maximum value for channel 1 is 0.789 mW/cm<sup>2</sup>.

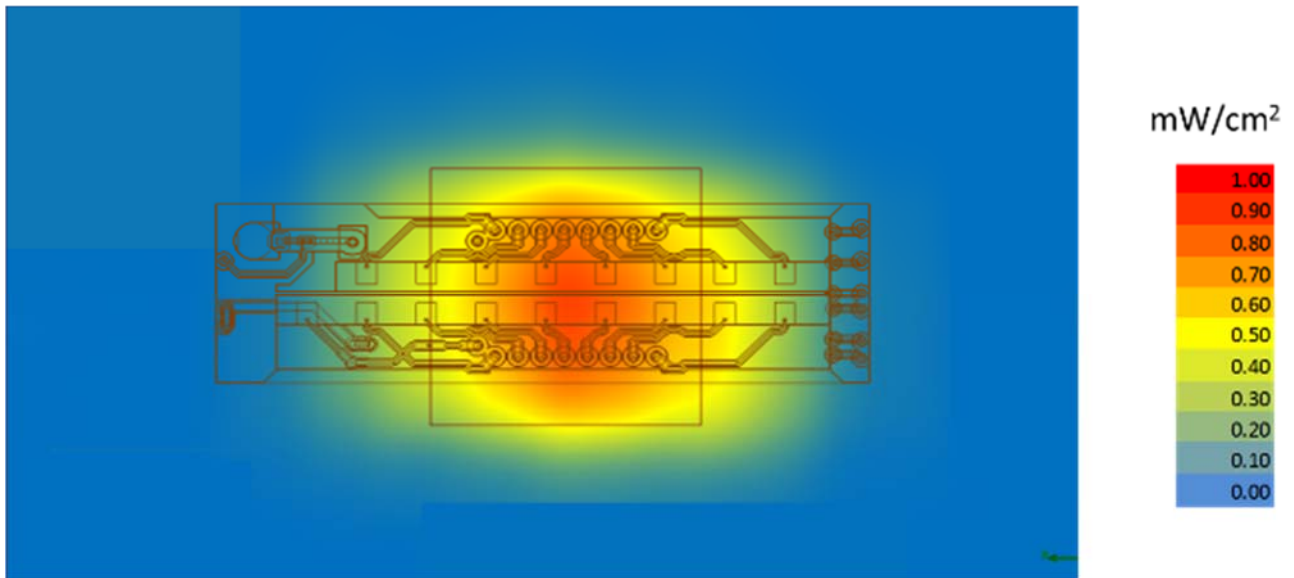


Figure 16 – Channel 2 Worst case - Integrated power over 1cm<sup>2</sup> an platform edge at 100% duty cycle

The maximum value for channel 2 is 0.862 mW/cm<sup>2</sup>.

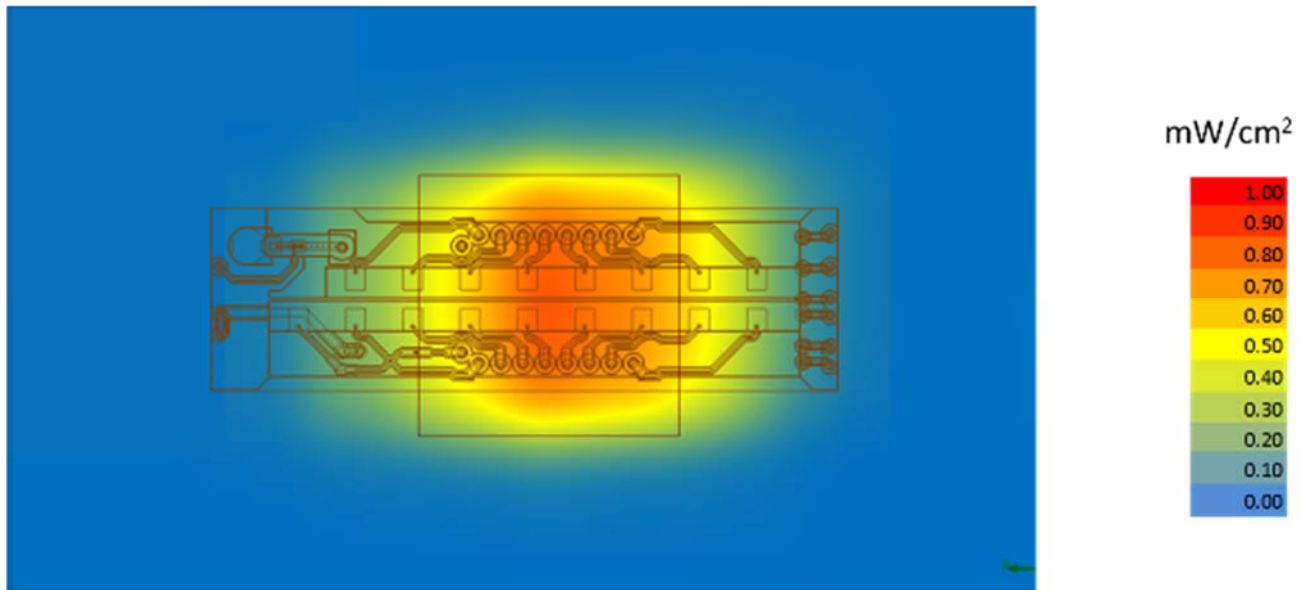


Figure 17 – Channel 3 Worst case - Integrated power over 1cm<sup>2</sup> an platform edge at 100% duty cycle

The maximum value for channel 3 is 0.826 mW/cm<sup>2</sup>.



## 4.5 Power density VS distance

The following figures show the worst case Z power-density integrated over 1 cm<sup>2</sup> using the worst case antenna phases (as described in section 3.4) computed by the simulation versus the distance from the platform boundary (0mm from the platform boundary is 2.03mm from the RFEM antenna – platform edge)

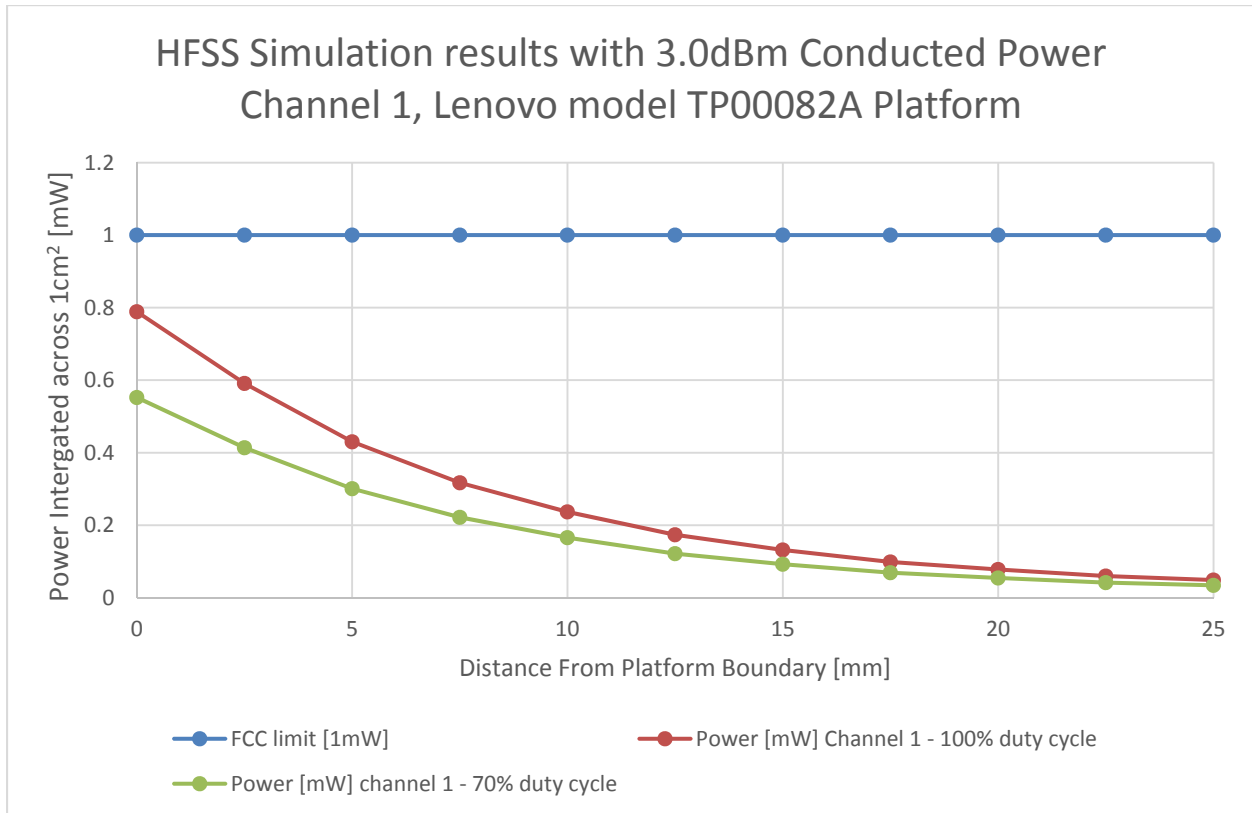
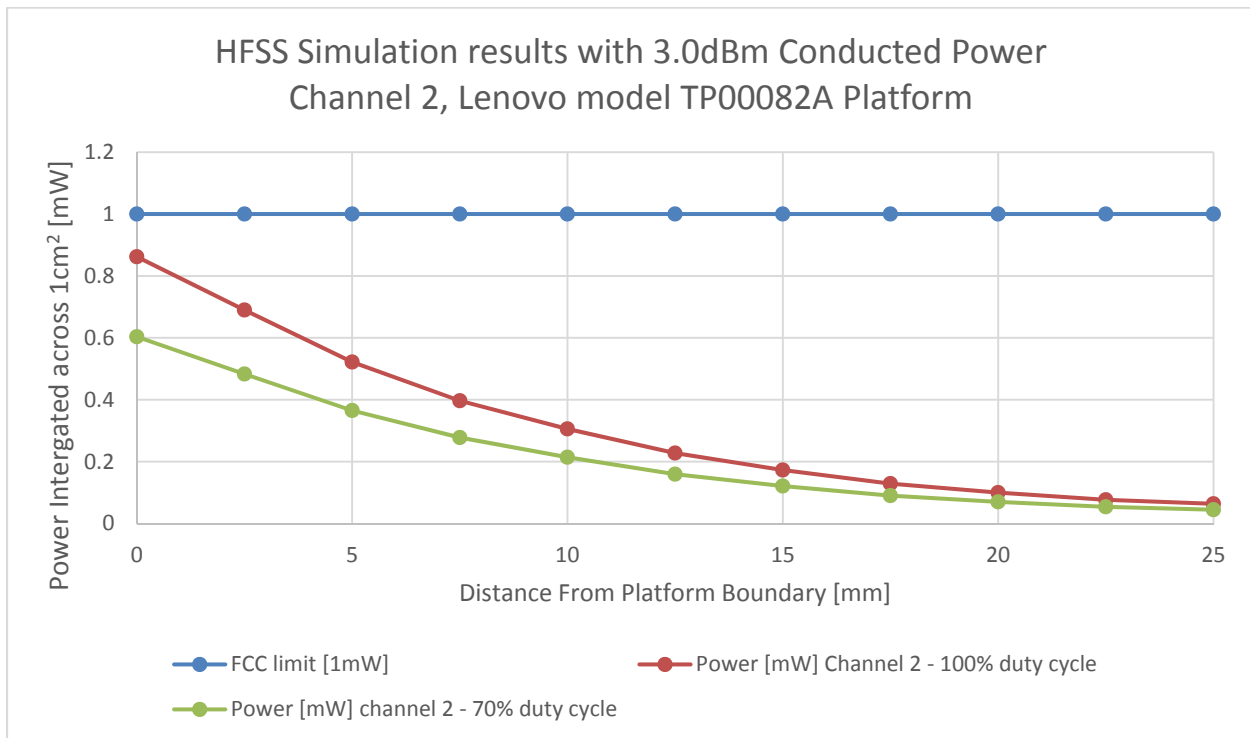
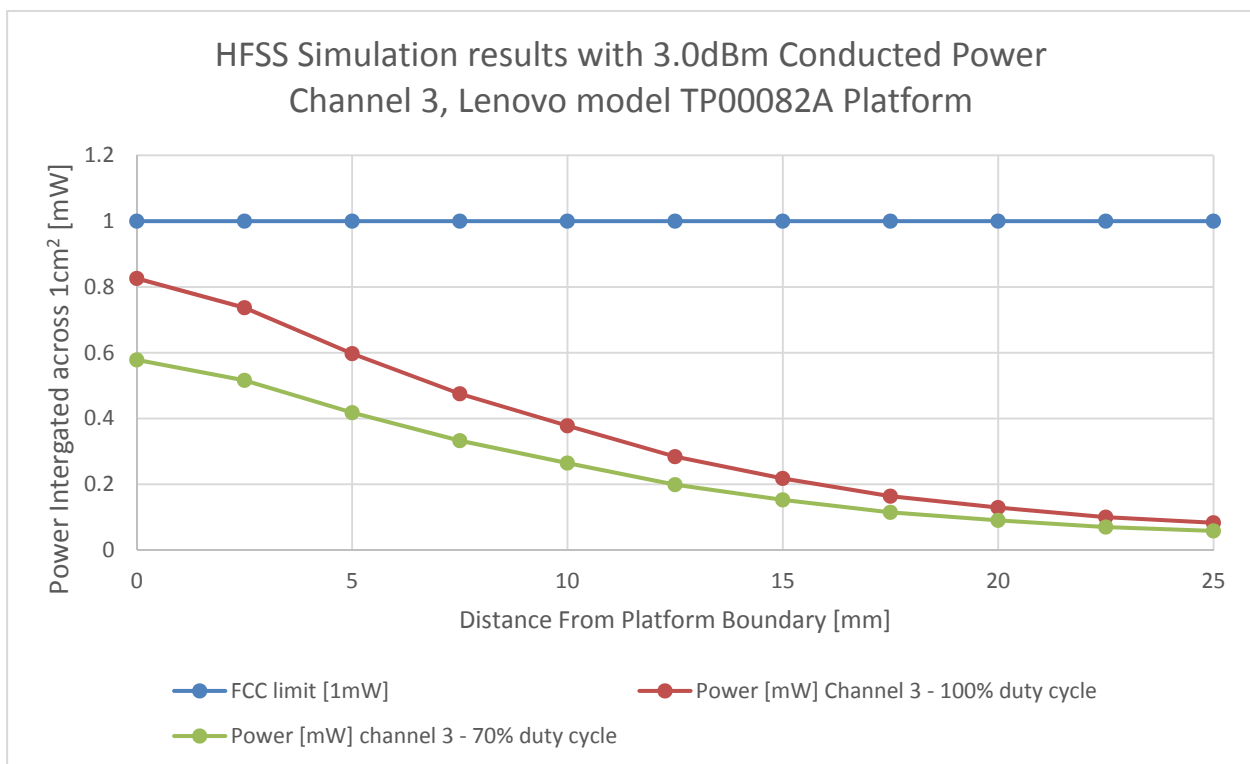


Figure 18 – HFSS Simulation results in Ch1



**Figure 19 – HFSS Simulation results in Ch2**



**Figure 20 – HFSS Simulation results in Ch3**





Notes for Figure 18 - Figure 20:

1. The worst case channel is channel 2.
2. The Maximum power density (spatially integrated over worst 1cm<sup>2</sup>) in channel 2 (worst case) is achieved at 0mm distance from the platform boundary and equals to 0.862mW/cm<sup>2</sup> over 100% duty cycle.
3. As explained in section 2.3, the Intel 11000D2W module is limited to Transmit at a duty cycle of 70% over 10sec. Therefore the maximum spatially integrated and time averaged power density over 1cm<sup>2</sup> is  $0.862 * 0.7 = 0.6034\text{mW/cm}^2$ .
4. Taking into account the ratios presented in Table 3 between the Z-component and the total power density, the integrated power densities values at zero distances become:

	Channel 1	Channel 2	Channel 3
<b>Integrated Power density in Z-direction</b> <i>(P<sub>z</sub>) [ mW/cm<sup>2</sup>]</i>	0.5523	0.6034	0.5782
<b>Corresponding Ratio</b> <i>(R)</i>	0.97	0.99	0.98
<b>Global Integrated Power density</b> <i>(P<sub>tot</sub>=P<sub>z</sub>/R) [ mW/cm<sup>2</sup>]</i>	0.5694	0.6095	0.5900

**Table 4 –Base plane integrated power density at zero distance**

Therefore, the worst case channel remains channel 2 and the maximum spatially integrated and time averaged total power density over 1cm<sup>2</sup> is  $0.6034 / 0.99=0.6095 \text{ mW/cm}^2$ .



## 5 Validation Simulation Model in Near-Field to Far-Field

---

Due to the lack of standardized code validation, benchmarking and uncertainty of the simulation software, the near field to far field results are included for the purpose of providing confidence for the software simulation model used and that the results produced were within an acceptable range when compared with the measured results. The error margins of all test results have been considered collectively by the FCC to determine compliance.

In order to validate the accuracy of the simulation we took a few measures, presented in this chapter, including correlation of the simulated power density in transition field to far-field against lab measurements. The same simulation was used for both power density estimation in near field (previous chapter) and transition field to far field correlation (this chapter).

### 5.1 Correlation of EIRP in the Near to Far Field

Note – the correlation of EIRP in near field to far field was done with conducted output power of 3dBm. This value was used for both lab measurements and simulation results.

#### 5.1.1 Far Field Boundary Calculation

Far field boundary can be estimated using *Fraunhofer distance* equation:

$$\text{FarFieldBoundary} = \frac{2d^2}{\lambda}$$

#### Equation 2 – Far field boundary calculation

In the RFEM, d (largest antenna dimension) = 16.1mm

Channel	$\lambda$ (wave length) [mm]	<i>Fraunhofer distance [cm]</i>
1	5.14	10.1
2	4.96	10.5
3	4.79	10.8

#### 5.1.2 Test laboratory

The measurements were done at the ISO 17025 accredited laboratory Intel Mobile Communications France S.A.S. with FCC registration number #3478.01 on Lenovo Model TP00082A platform with 11000D2W module. Data can be found in lab test report 15121701.TR01.



### 5.1.3 Correlation Of Measurements And Simulation

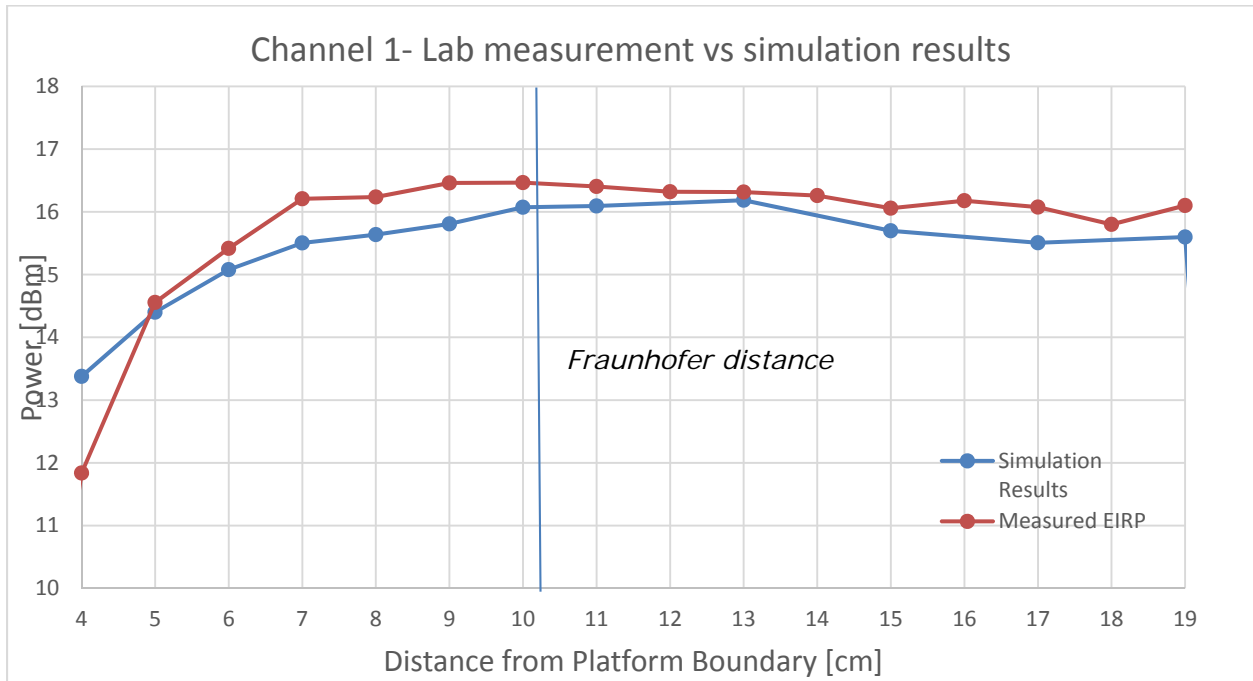


Figure 21 - Comparison of EIRP simulation to lab measurements – channel 1

Note: the measured EIRP values from the Lab Test Report are normalized to 100% duty cycle.

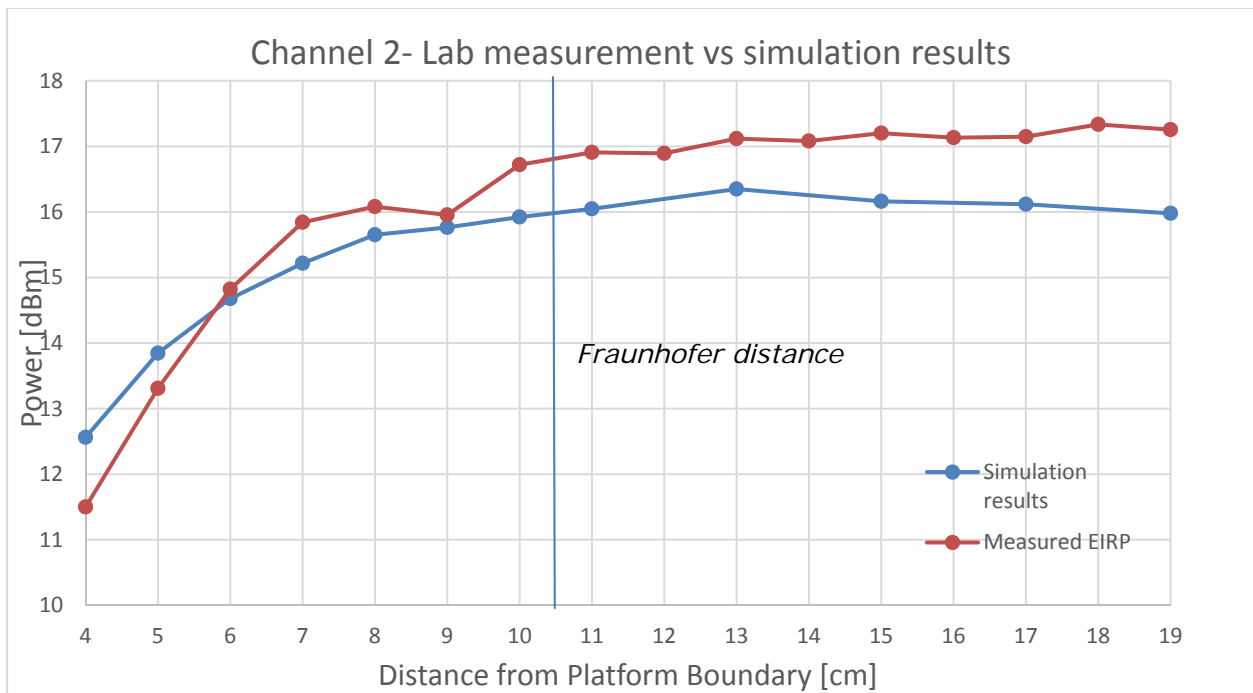
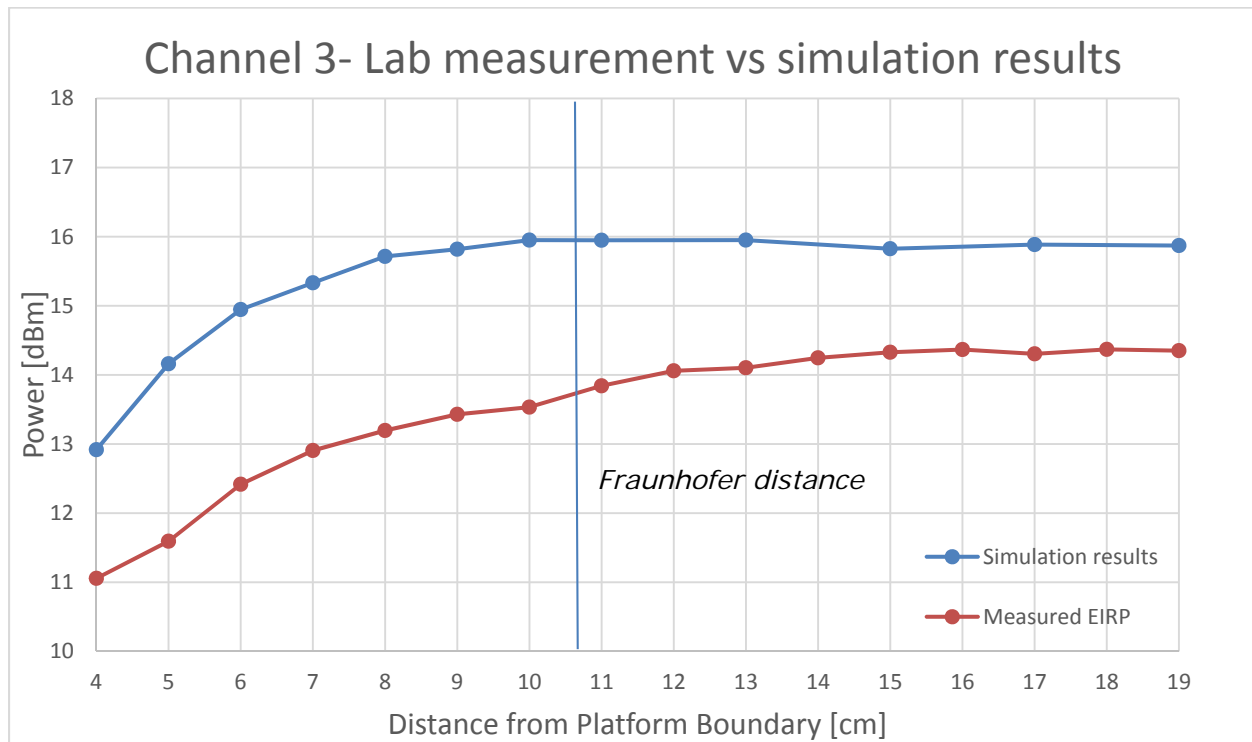


Figure 22 - Comparison of EIRP simulation to lab measurements – channel 2

Note: the measured EIRP values from the Lab Test Report are normalized to 100% duty cycle.



**Figure 23 - Comparison of EIRP simulation to lab measurements – channel 3**

Note: the measured EIRP values in the Lab Test Report are normalized to 100% duty cycle.

**Discussion – correlation results:**

The following observations can be made by looking at Figure 21 - Figure 23:

1. EIRP increased to a steady state, demonstrating we are in the near/transition field below 10cm (very close to the Fraunhofer distance).
2. Very good correlation can be seen in the graph shape and trends between lab measurements and simulation results.
3. Channel 1 measured data have very good correlation to simulation results, channel 2 measured data is slightly higher than simulated data (~1dB higher). Channel 3 measured data is ~1.5dB lower than simulated results.

Summary – as explained, good correlation can be seen between measured to simulated data.



### 5.1.4 Estimating conducted power level

Measured EIRP signal power can be used to estimate the conducted equivalent power that is fed to the antenna array. The estimation is done by subtracting the antenna gain from the estimated EIRP level in the higher distance range from the platform (12 – 19 cm).

The EIRP level is the same as reported in previous section. While the antenna gain is the antenna gain that is used in the 11000D2W modular approval.

Free Air Antenna Gain: Channel 1 – 15.30dBi, Channel 2 – 15.20dBi, Channel 3 – 14.8dBi

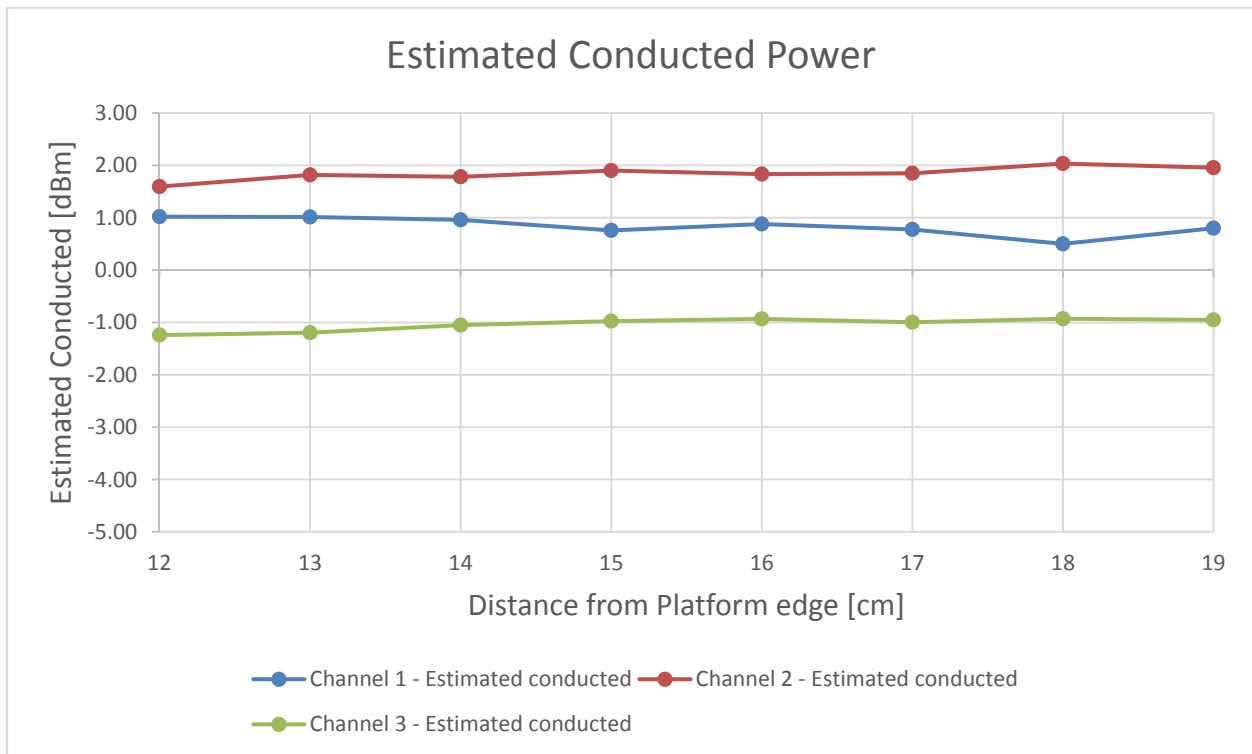


Figure 24 - Estimate conducted power from EIRP data

#### **Discussion – correlation results:**

Looking at Figure 24 one can see that the estimated conducted power is lower than the actual power level that was used. The tests were done with a conducted power of 3dBm while the estimated for channels 1 is ~ 1dBm, Channel 2 ~ 2dBm & channel 3 ~ -0.5dBm

1. The antenna gain that is used for this estimation is the modular antenna gain (antenna in free air). However the antenna that is embedded inside a platform has a platform loss that is typically in the vicinity of 1.0dB~2.0dB. This additional platform loss explains the power that is estimated for channel 1 & 2.
2. As seen in section 5.1.3, channel 3 is lower than the simulation expectations by ~1.5dB. This difference can be seen also in the estimation of the conducted power where channel 3 is lower than the assumed power by ~3.5dB (~1.5dB due to the fact that channel 3 is lower than simulation, additional ~2.0dB due to platform loss).

## 5.2 Simulating a Canonical Antenna Design

A simple patch antenna with Length = 7.5mm (GND plane length), and Lambda = 4.8mm, and was designed to work at 62.5GHz, as can be seen in the figure below.

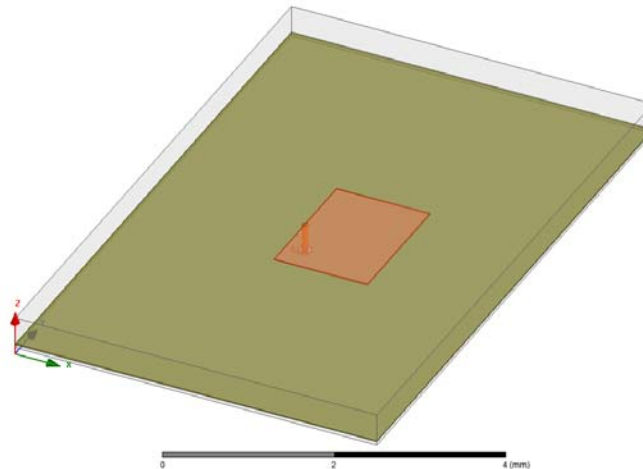


Figure 25 - Simulation of a single Patch antenna

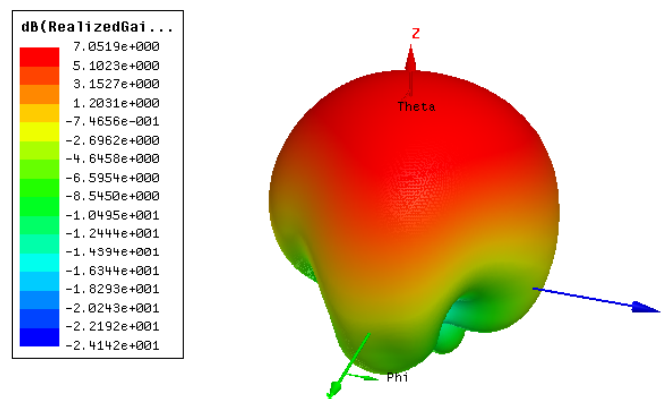
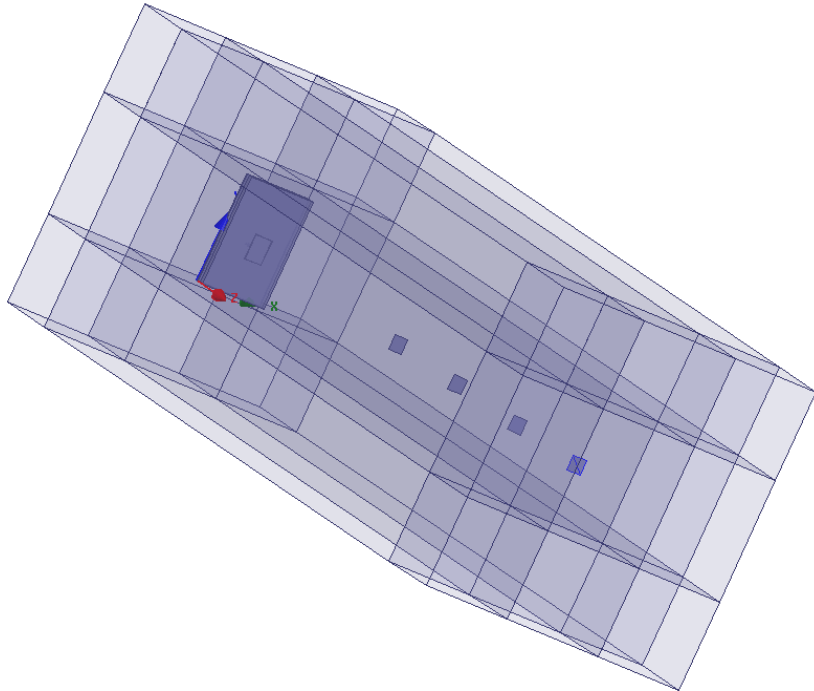


Figure 26 – Patch Antenna Gain

The simulated Far-Field Max Realized Gain [dBi] is 7.05[dBi], as simulated by far field simulation. The 7.05dBi gain was obtained using HFSS simulation using Far Field Gain option.

Theoretically patch antenna gives ~7-9dBi gain. The simulated patch antenna in the HFSS simulation is not a theoretical patch, it includes several “real life” non-idealities (width, size, feeding point etc). The 7.05 dBi Max Realized Gain is the gain obtained from HFSS simulation including those non-idealities.

A few test planes were integrated into the simulation at different far-field distances from the patch (shown below) for power density calculations:



**Figure 27 – Simulation 3D structure**

The distances between the patch and the test planes range from 24mm to 54mm.

To validate the numerical tool, the power density results at the test planes are translated into gain using omnidirectional power propagation and compared to far field gain according to simulation (table below).

The table below summarizes the results:

Far Field Distance	$P_{omni} = \frac{P}{4\pi R^2} \left[ \frac{W}{mm^2} \right]$	Power Density from simulation $\left[ \frac{W}{mm^2} \right]$	Gain calculation from power density [dBi]
24mm	1.34e-4	6.70e-4	6.99
29mm	9.11e-5	4.61e-4	7.04
34mm	6.59e-5	3.38e-4	7.10
44mm	3.91e-5	2.03e-4	7.15
54mm	2.59e-5	1.35e-4	7.17

**Table 5 – Gain calculation from power density per several distances**

Where P is the simulated radiated power and R is the distance from the patch to the test plane.

The table above shows excellent correlation between the Patch antenna gain calculated from power density, to the Far-Field Max realized gain (7.05[dBi]). This is also depicted in the figure below:

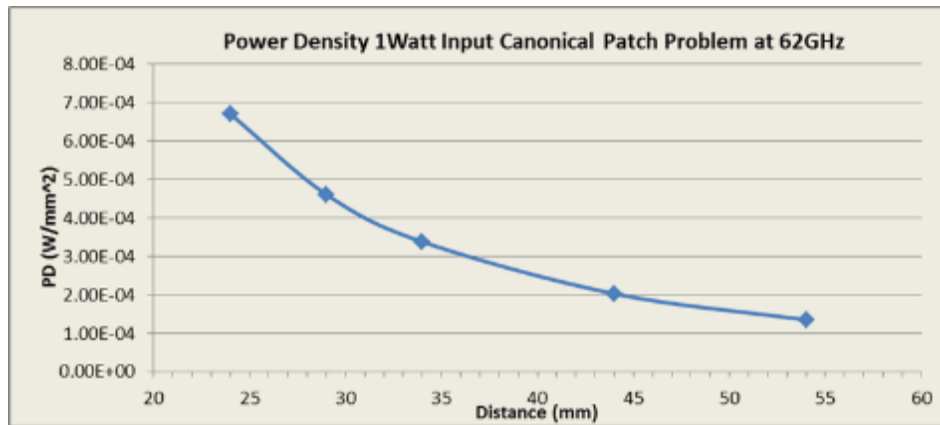


Figure 28– Power Density of Canonical Patch Antenna





## 6 Summary

---

Due to the lack of standardized code validation, benchmarking and uncertainty of the simulation software, the near field to far field results are included for the purpose of providing confidence in the software simulation model used and that the results produced were within an acceptable range when compared with the measured results. The error margins of all test results have been considered collectively by the FCC to establish confidence for the accuracy of the HFSS simulation.

The following table summarizes the simulation results in the near field of Intel 11000D2W module, embedded in Lenovo Model TP00082A:

Parameter	Value
Total conducted power	3.0 dBm
Maximum TX duty-cycle	70%
Maximum spatially integrated and timed average power density, over 1cm <sup>2</sup> and 10 seconds	0.6034mW/cm <sup>2</sup>
Maximum spatially integrated and timed average power density, over 1cm <sup>2</sup> and 10 seconds taking into account the ratios presented in Table 3. (see details in Table 4)	0.6095mW/cm <sup>2</sup>

**Table 6 – Summary of simulation results for RF exposure compliance**

Therefore Intel 11000D2W module, embedded in Lenovo Model TP00082A, complies with FCC rule parts §2.1093 and §15.255(g).